Published in final edited form as:

Genes Immun. 2019 March ; 20(3): 181–197. doi:10.1038/s41435-018-0023-2.

Human *IL12RB1* expression is allele-biased and produces a novel IL12 response regulator

Allison E. Reeme[†], **Tiffany A. Claeys**[†], **Praful Aggarwal**[‡], **Amy J. Turner**[‡], **John M. Routes**[§], **Ulrich Broeckel**[‡], and **Richard T. Robinson**[†,¶]

[†]Department of Microbiology and Immunology, Section of Genomic Pediatrics and Children's Research Institute

[‡]Department of Pediatrics, Section of Genomic Pediatrics and Children's Research Institute

[§]Department of Pediatrics, Section of Asthma, Allergy and Clinical Immunology, The Medical College of Wisconsin, Milwaukee, WI 53226

Abstract

Human *IL12RB1* is an autosomal gene that is essential for mycobacterial disease resistance and T cell differentiation. Using primary human tissue and PBMCs, we demonstrate that lung and T cell *IL12RB1* expression is allele-biased, and the extent to which cells express one *IL12RB1* allele is unaffected by activation. Furthermore, following its expression the *IL12RB1* pre-mRNA is processed into either *IL12RB1* Isoform 1 (IL12Rβ1, a positive regulator of IL12-responsiveness) or *IL12RB1* Isoform 2 (a protein of heretofore unknown function). T cells' choice to process pre-mRNA into Isoform 1 or Isoform 2 is controlled by intragenic competition of *IL12RB1* exon 9-10 splicing with *IL12RB1* exon 9b splicing, as well as an *IL12RB1* exon 9b-associated polyadenylation site. Heterogeneous nuclear ribonucleoprotein H (hnRNP H) binds near the regulated polyadenylation site, but is not required for exon 9b polyadenylation. Finally, microRNA-mediated knockdown experiments demonstrated that *IL12RB1* Isoform 2 promotes T cell IL12 responses. Collectively, our data support a model wherein tissue expression of human *IL12RB1* is allele-biased and produces an hnRNP H bound pre-mRNA, the processing of which generates a novel IL12 response regulator.

Keywords

Allele-bias; Monoallelic; hnRNP; *IL12RB1*; mycobacteria

INTRODUCTION

IL12RB1 is a Mendelian susceptibility to mycobacterial disease (MSMD) gene that promotes IFNγ immunity and mycobacterial disease resistance[1]. In the absence of a

[¶]Corresponding author: rrobinson@mcw.edu; Phone: 414-955-2976; Fax: 414-955-6535.

CONFLICT OF INTEREST

The authors declare no competing financial interests in relation to the work described.

functional *IL12RB1* allele, individuals are susceptible to lung infection with tuberculous and nontuberculous *Mycobacteria* species, and T cells are insensitive to the cytokines IL12 and IL23[2, 3]. Aberrant splicing is among the most common causes of *IL12RB1* deficiency[4]. In addition to mycobacterial disease, common *IL12RB1* haplotypes also associate with measles vaccine efficacy[5, 6], pediatric asthma susceptibility[7, 8], and food allergy among breast-fed toddlers[9]. Given the impact of *IL12RB1* on multiple diseases, it is important to identify and understand the factors governing *IL12RB1* expression, splicing and function.

T cells express two major *IL12RB1* isoforms as a result of alternative mRNA processing[3]. The first isoform (IL12Rβ1, or Isoform 1) is a cell surface receptor that binds the IL12p40 domain of IL12/IL23[10–12], and cooperates with co-receptors IL12Rβ2 or IL23R to initiate intracellular STAT signaling[3]. An important consequence of IL12/IL23 signaling is increased secretion of IFNγ[10, 13], which limits mycobacteria survival in multiple organs[14, 15]. The second isoform (Isoform 2) retains the IL12p40-binding domains of Isoform 1, but lacks the Isoform 1 transmembrane domain and localizes to an intracellular reticulum[16]. Based on these data we initially predicted that Isoform 2 is non-functional protein located distal to extracellular cytokine[16]; however, subsequent studies using IL12Rβ1ΔTM$^{-/-}$ mice (IL12Rβ1ΔTM is the mouse homolog of human Isoform 2) support a different model wherein Isoform 2 functions to promote IL12 responses and T_H1 development during experimental tuberculosis[17]. The factors affecting T cells' decision to transcribe and alternatively process *IL12RB1* mRNA into Isoform 1 or Isoform 2 are unknown, nor has a role for human *IL12RB1* Isoform 2 been empirically determined.

Among autosomal genes that regulate T cell function, the factors affecting mRNA processing include monoallelic or allele-biased expression[18], and heterogeneous nuclear ribonucleoproteins[19, 20]. Allele-biased expression occurs when only one copy of a gene (either the maternal- or paternal-derived allele) is predominately transcribed, while the other allele is transcriptionally silent. Allele-biased expression is used by T cells to regulate transcription of genes that affect their thymic development[21, 22], as well as the genes that affect their cytokine responses[23–30]. After T cells transcribe these and other genes, heterogeneous nuclear ribonucleoproteins (hnRNPs) physically associate with the pre-mRNA and participate in alternative splicing, polyadenylation, nuclear export and localization to ribosomes[20]. There are approximately twenty major hnRNPs in humans (hnRNP A1 – U) which vary in size, RNA recognition motif, and function[31]. Among the major hnRNPs that regulate alternative splicing in lymphocytes are hnRNPs A/B[32], hnRNP F[33], hnRNP H[33], hnRNP L[34–38], hnRNP LL[38–41] and hnRNP U[42].

Here we report the results of experiments which were designed to identify factors regulating *IL12RB1* mRNA expression and processing, as well as determine Isoform 2′s function in the context of an IL12 response. Using primary tissues and T cell lines, we demonstrate that *IL12RB1* expression is allele-biased, and T cells' decision to produce either Isoform 1 or Isoform 2 is regulated by intragenic competition between *IL12RB1* exon 9-10 splicing and *IL12RB1* exon 9b splicing / polyadenylation. We also demonstrate that IL12-dependent IFNγ expression is attenuated in T cells that are transduced with Isoform 2 specific microRNAs. Collectively, these data support a model wherein human *IL12RB1* pre-mRNAs are primarily transcribed from one allele, and that alternative processing of these pre-

mRNAs is modulated an *IL12RB1* exon 9b polyA site that is upstream of hnRNP H binding. A consequence of this alternative processing is the production of a novel IL12 response regulator.

RESULTS

Expression of IL12RB1 in human lung tissue is allele-biased

IL12RB1 expression in the lung is important for mycobacterial disease resistance[1]. To determine if *IL12RB1* expression in the lungs is allele biased, we deep sequenced *IL12RB1* gDNA and mRNA from human lung specimens, determined each donor genotype at eleven polymorphic positions in the *IL12RB1* gene, and then used this information to educe the allelic origin of *IL12RB1* mRNA in the same specimen. Deep sequencing was done using the Ion Torrent platform as previously described[43]; the average *IL12RB1* gDNA and mRNA read depths across all samples were 2907× and 13222×, respectively (supplemental TABLE S2). To determine a donor's genotype, we queried their gDNA sequence at eleven polymorphic sites in the *IL12RB1* gene (chromosome 19 positions 18170384, 18170755, 18180413, 18180451, 18186575, 18186618, 18188408, 18191664, 18192977, 18194255 and 18197635), and whether they were heterozygous (i.e. each *IL12RB1* allele had a different nucleotide at that position) or homozygous (i.e. both *IL12RB1* alleles had the same nucleotide at that position). Donor gDNA that was heterozygous at a given site would have two nucleotides that each theoretically comprise 50% of all the reads, while a donor who was homozygous at a given site would have one nucleotide that theoretically comprises 100% of all reads. If a donor was heterozygous, we could determine if their *IL12RB1* mRNAs represented both alleles equally (indicating biallelic expression) or predominantly represented one allele (indicating allele-biased transcription) by comparing the allele read frequency among gDNA and mRNA reads. The allele read frequency (ARF) is a numerical value that indicates the representation of a given nucleotide among all the reads of a specific position in the gDNA (ARF^{gDNA}) or mRNA (ARF^{mRNA}).

The results of our analyzing eight specimens in this manner are depicted in FIG 1. Four donors were homozygous at each polymorphic site, and thus could not be used to determine if *IL12RB1* transcription was allele-biased (FIG 1A). Four other donors were heterozygous at one or more polymorphic sites in the *IL12RB1* gene, and thus could be used to determine if mRNAs present in the same tissue were monoallelic or biallelic in origin (FIG 1B). Donor S3 was polymorphic at gDNA position 18170384; although the ARF^{gDNA} values for both alleles were roughly equal (G, 48%; A, 52%), the ARF^{mRNA} values were not (G, 100%; A, 0%). The same result was true for Donor N3. Donor N5 was polymorphic at six gDNA positions (18170384, 18180413, 18180451, 18186575, 18186618 and 18191664); the range of ARF^{gDNA} values for these six positions was consistent with equal allelic representation (44%-56%), while the ARF^{mRNA} values were biased towards one allele (82%-100%) at the expense of the other allele (0-18%). Donor S1 was polymorphic at seven gDNA positions (18170384, 18180413, 18180451, 18186575, 18186618, 18188408 and 18197635); as with Donor N5, the range of ARF^{gDNA} values for these seven positions was consistent with equal allelic representation (41%-59%), while the ARF^{mRNA} values were biased towards one allele (97%-100%) at the expense of the other allele (0-3%). When these ARF^{gDNA} and

ARF^{mRNA} data from FIG 1B are pooled and plotted, there was a significant difference in the regression pattern of the two data sets (FIG 1C). Namely, while *IL12RB1* ARF^{gDNA} values displayed a Gaussian distribution (mean=50%), the *IL12RB1* ARF^{mRNA} values were non-Gaussian and bifurcated toward either 0% or 100% representation, which is consistent with monoallelic gene expression[18].

To ensure that our deep sequencing results were reflected in individual mRNA clones, lung mRNA was used to generate an *IL12RB1* cDNA library, from which individual clones were randomly selected for Sanger sequencing Donor S1 lung mRNA was chosen to generate this library because their gDNA was heterozygous for more *IL12RB1* single nucleotide polymorphisms (SNPs) than any other donor (FIG 1B). Each clone within a library contained the entire length of the *IL12RB1* cDNA (~2,000 bp); ten individual clones were randomly selected and Sanger sequenced 2-3 times with overlapping primer sets. To educe each cDNAs clone's allele-of-origin, its Sanger sequencing trace was visually inspected at six cDNA positions (63, 531, 705, 748, 1158 and 1196) that correspond to six gDNA positions that are polymorphic in Donor S1 gDNA (18197635, 18188408, 18186618, 18186575, 18180451 and 18180413). This analysis demonstrated that of ten *IL12RB1* cDNA clones, all originated from the same *IL12RB1* allele. Namely, each cDNA clone encoded the following SNPs: 18197635C, 18188408G, 18186618A, 18186575C, 18180451T and 18180413G (FIG 1D–E). This is the same allele that we concluded (based on Ion Torrent data) was preferentially expressed in Donor S1 (FIG 1B). Collectively, these data demonstrate that *IL12RB1* expression in human lung tissue is allele biased, as determined by Ion Torrent and Sanger sequencing.

Expression of IL12RB1 in human T cells is allele-biased

Based on the above studies, we next wished to determine if *IL12RB1* expression is allele biased in T cells, since T cell *IL12RB1* expression promotes lung mycobacterial disease resistance[44]. *IL12RB1* expression is required for $CD4^+$ and $CD8^+$ T cell differentiation in humans and mouse models[1, 44, 45], and the two most common *IL12RB1* haplotypes ("QMG" and "RTR") encode receptors that differ in IL12-sensitivity[4, 46]. The three SNPs which comprise the QMG and RTR haplotype are located at gDNA positions 18186618, 18180451 and 18180413 (indicated by asterisks in FIG 1A). To determine if PBMC and T cell *IL12RB1* expression is allele biased, PBMCs from nine healthy adult donors were isolated and cultured in the presence of PHA; $CD4^+$ and $CD8^+$ T cells were purified from PBMC preparations using an antibody-conjugated bead system, both before and after PHA-stimulation. The gDNA of each PBMC preparation was used for PCR amplification of *IL12RB1* exon 10, which contains two constituent SNPs of the QMG allele (18180451T and 18180413G) or RTR allele (18180451C and 18180413C); exon 10 amplicons were Sanger sequenced to determine if the donor was heterozygous or homozygous for the QMG and/or RTR haplotype. The Sanger sequence trace of a heterozygous donor is shown in FIG 2A, demonstrating the detection of two nucleotides at each position in the QMG/RTR haplotype. The mRNA of each PBMC, $CD4^+$ and $CD8^+$ T cell preparation was used to generate and analyze individual *IL12RB1* cDNA libraries, in the same manner as was done for lung tissue (FIG 1D–E).

The results of our analyzing nine donors in this manner are shown in FIG 2. Three PBMC donors were homozygous for the QMG or RTR haplotype, and thus could not be used to determine if *IL12RB1* transcription was allele-biased (data not shown). Six PBMC donors were heterozygous for the QMG and RTR haplotype, and thus could be used to determine the allelic origin of each *IL12RB1* cDNA clone (FIG 2A–B). Among the *IL12RB1* cDNA clones from unstimulated (-PHA) PBMCs, 83% were derived from the QMG allele; this frequency was virtually unaffected in stimulated (+PHA) PBMCs (FIG 2C). Among the *IL12RB1* cDNA clones from $CD4^+$ and $CD8^+$ T cells, 100% were derived from the QMG allele, regardless of stimulation (FIG 2D). Collectively, these data demonstrate that *IL12RB1* expression in human PBMCs and T cells is allele-biased.

IL12RB1 isoform production is due to intragenic competition between exons 9/10 splicing and exon 9b splicing/polyadenylation

After an *IL12RB1* allele is expressed, T cells must choose whether to process the *IL12RB1* pre-mRNA into Isoform 1 (the function of which is to promote IL12 responses) or Isoform 2 (the function of which is heretofore unknown). The elements which govern this processing choice are unknown. To identify elements within *IL12RB1* that govern its alternative processing, and to determine the function of Isoform 2 in the context of IL12 responses, we used the Jurkat cell model of primary human T cells. Jurkat cells are a leukemic human T cell line that recapitulates many aspects of primary human T cells[47], including allele-biased *IL12RB1* expression (FIG 3A) and processing *IL12RB1* pre-mRNA into Isoform 1 and Isoform 2 (FIG 3B).

The production of Isoform 1 (Iso1) results from the splicing of *IL12RB1* exons 1-17, with skipping of exon 9b (FIG 4A top), while production of Isoform 2 (Iso2) results from splicing *IL12RB1* exons 1-9 and the alternate 3′ exon 9b (FIG 4A bottom) and subsequent use of a 9b-specific polyadenylation site[16]. To better understand the alternative splicing of *IL12RB1* mRNA exon 9b, we generated a series of *IL12RB1* minigenes that lacked regions with predicted regulatory sequences (FIG 4B), transfected each minigene into the Jurkat T cell line, and then measured the expression of minigene-derived Iso1 and Iso2 mRNA. To generate a wild type *IL12RB1* minigene that recapitulated endogenous *IL12RB1* mRNA processing, the 2804 bp sequence comprising *IL12RB1* exons 9→9b→10 was cloned into vector p3XFLAG-CMV7.1 (p*B1*$^{9–10}$, FIG 4B). The rationale for this design was that most examples of alternative splicing involve *cis*-elements that are proximal to the affected exon, so we predicted that a minigene comprising *IL12RB1* exons 9→9b→10 would harbor the *cis* elements necessary for alternative processing of *IL12RB1* into Iso1 and Iso2. Iso2 uses the polyadenylation (polyA) site within exon 9b whereas Iso1 uses the polyA site provided by the vector, downstream of the *IL12RB1* insert. In the event that sequences outside of *IL12RB1* exons 9→9b→10 contribute to alternative splicing of Iso1 or Iso2, we also generated a minigene that included intron 10 and exon 11 (p*B1*$^{9–11}$, FIG 4B).

The results of transfecting p*B1*$^{9–10}$ and p*B1*$^{9–11}$ into Jurkat T cells are shown in FIG 4C, and demonstrate that p*B1*$^{9–10}$ expressed two isoforms of *IL12RB1* corresponding to Iso1 and Iso2, independent of PHA stimulation (FIG 4C, lanes 3–4). p*B1*$^{9–11}$ also recapitulated endogenous processing of *IL12RB1* into Iso1 and Iso2, albeit this minigene also produced a

minor Iso1 splice variant consistent with splicing from exon 9 to exon 11 (Iso1Δex10) that we have previously observed in primary T cells (FIG 4C, lanes 5–6)[16]. As anticipated, no isoforms were expressed from our empty vector control (FIG 4C lane 7), or cDNA prepared without RT (FIG 4C lane 2). The data in FIG 4C thus demonstrate that *IL12RB1* minigenes recapitulate endogenous *IL12RB1* mRNA processing. Based on alternative splicing literature[48–50], we generated *IL12RB1* minigene deletion mutants lacking the exon 9b polyA site (ΔpolyA, FIG 4B), exon 9b polyA site and exon 10 (ΔpolyAΔex10, FIG 4B), exon 9b (Δex9b, FIG 4B), and exon 10 (Δex10, FIG 4B). Each minigene deletion mutant was then transfected into Jurkat T cells, and the expression of minigene-derived Iso1 and Iso2 was assessed. The data from these experiments are shown in FIG 4D, and demonstrate that preferential expression of Iso1 is unaffected by exon 9b polyA deletion (compare FIG 4D lanes 4 & 5), nor is it affected by the deletion of exon 9b (compare FIG 4D lanes 4 & 7). However, deletion of exon 10 - either alone or in combination with the exon 9b polyA site – results in enhanced expression of Iso2 (compare FIG 4D lane 4 to lanes 6 & 8). Minigene-derived Iso1 and Iso2 mRNAs were not observed in mock-treated or minus-RT controls (FIG 4D, lanes 2–3). Collectively, these data show that i) the exon 9b polyA site is needed for splicing to the exon 9b 3′ splice site (ΔpA), ii) the exon 9b 3′ss is functional in the absence of competition with exon 10 (ΔpAex10), and iii) the exon 9b polyA site is functional in the absence of competition from exon 9 to 10 splicing (Δex10), and indicate that competition between splicing of exons 9 and 10 with exon 9b splicing / polyadenylation underlies isoform production.

hnRNP H binds to IL12RB1 pre-mRNAs via G-tracts that are downstream of the exon 9b polyA site

Heterogeneous nuclear ribonucleoprotein H (hnRNP H) is a ubiquitously expressed regulator of alternative splicing and polyadenylation that binds mRNA via poly-guanine sequences (G-tracts)[51–59]. Three consecutive guanines are sufficient for binding hnRNP H[60], which in turn can influence spliceosome activity or polyadenylation. Since there are five G-tracts downstream of the regulated *IL12RB1* poly(A) site that are putative hnRNP H binding sites (FIG 5A), we hypothesized that hnRNP H-bound G-tracts contribute to the alternative processing of *IL12RB1*. To test this hypothesis, we first determined if hnRNP H binds *IL12RB1* transcripts via the G-tracts depicted in FIG 5A. Specifically, *in vitro* transcription (IVT) was used to produce 84 nt *IL12RB1* RNAs that harbor each G tract, as well as RNA with mutations in the G-tracts that are known to abolish hnRNP H binding (i.e. GGG→GUG; mutated G-tracts depicted in FIG 5A). RNAs generated using radiolabeled ^{32}P-nucleotides were incubated with HeLa cell nuclear extract, UV-crosslinked to associated proteins, and immunoprecipitated using anti-hnRNP H or preimmune sera. Immunoprecipitated protein/RNA complexes were resolved via SDS-PAGE and visualized via ^{32}P-autoradiography. As a positive control for hnRNP binding we used the sense strand of a 118 nt Rous sarcoma virus RNA (RSV^{Sense}) that is known to bind hnRNP H[52]; the antisense strand of the same RSV RNA (RSV^{AS}) served as a negative control for hnRNP H binding.

The results of this analysis are shown in FIG 5B, and demonstrated that anti-hnRNP H immunoprecipitates hnRNP H cross-linked to RNA using wild type *IL12RB1* RNA

(compare FIG 5B lanes 1 & 8); the size of this band is similar to that immunoprecipitated from two independent positive controls from Rous sarcoma virus (RSV^{Sense1} and RSV^{Sense2}, lanes 3 and 5) and is consistent with hnRNP H (compare FIG 5B lanes 1 &3), and is absent in negative controls including RSV^{AS} (FIG 5B lanes 4, 6-11). Importantly, anti-hnRNP H fails to immunoprecipitate cross-linked hnRNP H using mutant G-tract *IL12RB1* RNA (FIG 5B lane 2). Based on the data in FIG 5B, we conclude that hnRNP H physically associates with *IL12RB1* RNAs via G-tracts that are downstream of its regulated poly(A) site. Since hnRNP H regulates pre-mRNA processing upon G-tract association[56], we predicted that G-tract mutations would affect the relative levels of *IL12RB1* Iso1 and Iso2. To test this hypothesis, we transfected Jurkat T cells with either p$B1^{9–10}$ or p$B1^{9–10}$mutG-tract, and then measured the expression of Iso1 and Iso2 mRNAs from each minigene. The results of this analysis are shown in FIG 5C–D and demonstrate that when the *IL12RB1* G-tracts were mutated, T cells continued to preferentially express Iso1 over Iso2 (compare FIG 5C lanes 3–6); quantifying the ratio of plasmid-derived *IL12RB1* Iso1:Iso2 levels also demonstrated no significant difference between p$B1^{9–10}$ or p$B1^{9–10}$mutG-tract (FIG 5D). Similar results were obtained from Jurkat T cells transfected with p$B1^{9–11}$ and p$B1^{9–11}$mutG-tract (p$B1^{9–11}$ with the G-tract mutations) (FIG 5C lanes 7–10, 5D). Collectively, these data demonstrate that hnRNP H binds to the G-tracts immediately downstream of *IL12RB1* exon 9b, but that *IL12RB1* pre-mRNA processing is G-tract independent.

Human IL12RB1 Isoform 2 positively regulates IL12-dependent IFNγ expression

The mouse homolog on human Iso2 (i.e. IL12Rβ1ΔTM) is a positive regulator of T cell responses to IL12[17]. Whether human Iso2 serves the same function has not yet been determined. Based on our previous studies of IL12Rβ1ΔTM knockout mice[17], we hypothesized that human Iso2 positively regulates T cell responses to IL12. To test this hypothesis, we transduced Jurkat T cells with microRNAs (miRs) that we engineered to knockdown Iso2 mRNA without affecting Iso1 mRNA; transductants were then stimulated in the presence or absence of IL12, and their expression of IFNγ was used as readout of IL12-responsiveness. The five miRs we generated are depicted in FIG S1A; each miR was designed to target an mRNA sequence that is encoded by *IL12RB1* Exon 9b and thus specific to Iso2 (FIG S1B). Of these five miRs (miR$^{\pi}$, miR$^{\phi}$, miR$^{\sigma}$, miR$^{\mu}$ and miR$^{\varepsilon}$), validation studies demonstrated that only two (miR$^{\sigma}$ and miR$^{\mu}$) could knockdown Iso2 mRNA expression to ≤10% of control levels (FIG S1C–D). Based on these validation studies, lentiviral vectors were generated and used to transduce Jurkat T cells with a cDNA encoding GFP and miR$^{\sigma}$, miR$^{\mu}$ or miR^{Neg} (a nonspecific control). Transductants were purified via FACS based on GFP expression, and stimulated for two days in media containing PHA alone (-IL12), PHA and 1 ng/mL IL12 ($IL12^{Lo}$), or PHA and 10 ng/mL IL12 ($IL12^{Hi}$). The cells and their supernatants were then collected and used for RT-PCR and ELISA analysis, respectively.

Relative to Jurkat cells that were either non-transduced or miR^{Neg}-transduced, Iso2 mRNA expression was not observed in cells transduced with either miR$^{\sigma}$ or miR$^{\mu}$ (FIG 6A, lower band), indicating efficient Iso2 knockdown. Importantly, Iso1 mRNA expression was intact in cells transduced with miR$^{\sigma}$ or miR$^{\mu}$, whether observed visually (FIG 6A, higher band) or

measured quantitatively (FIG 6B). No significant differences in Iso1 expression existed between miR^{Neg}, miR^{σ} or miR^{μ} groups (FIG 6B). Unexpectedly, all miR-transductants expressed higher levels of Iso1 relative to non-transduced cells (FIG 6B). We concluded from the data in FIG 6A–B that both miR^{σ} and miR^{μ} behaved as anticipated, and knocked down Iso2 mRNA without affecting Iso1 mRNA. We then moved forward and measured IFNγ mRNA and protein expression by the same cell preparations. The data from these measurements are shown in FIG 6C–D, and demonstrate that knockdown of Iso2 attenuates IL12-dependent IFNγ expression. Namely, miR^{Neg} transductants responded to IL12 in a dose-dependent manner by increasing IFNγ mRNA transcription (albeit variable), whereas miR^{σ} or miR^{μ} transductants did not (FIG 6C). miR^{Neg} transductants also (and less variably) responded to IL12 in a dose-dependent manner by increasing IFNγ secretion, whereas miR^{σ} or miR^{μ} transductants did not (FIG 6D). Collectively, these data demonstrate that IL12-elicited IFNγ transcription and secretion is attenuated in the absence of *IL12RB1* Iso2.

DISCUSSION

The gene *IL12RB1* regulates multiple aspects of human immunity, including resistance to tuberculous and nontuberculous mycobacterial pathogens[2]. Our current understanding of *IL12RB1* is primarily derived from studies of *IL12RB1*-deficient children, who are otherwise healthy prior to mycobacteria exposure[61]. The propensity of *IL12RB1*-deficient children to develop mycobacterial disease is commonly interpreted to reflect the absence of Isoform 1 (i.e. IL12Rβ1), which is an integral membrane protein that associates with IL12Rβ2 and IL23R to form the IL12- and IL23-signaling complex, respectively[3]. IL12 and IL23 both promote IFNγ secretion[10, 13], which in turn activates macrophages and limits mycobacteria survival[14, 15]. However, we and others have reported that a second *IL12RB1* isoform (Isoform 2) exists in mice and humans as the result of alternative splicing[16, 17, 62–64]. Although the mouse homolog of Isoform 2 functions in mice to promote IL12-dependent IFNγ secretion[17], its function in humans has heretofore been untested. There is also little to no information regarding the factors governing *IL12RB1* expression in immunocompetent individuals. It was for these reasons that we undertook the studies described above, which we believe support the model depicted in FIGURE 7.

Human *IL12RB1* is located on chromosome 19[65], and with rare exceptions each person inherits two functional *IL12RB1* alleles (FIG 7A). We can say this with certainty given the rarity of Mendelian susceptibility to mycobacterial disease (MSMD), which is a primary immunodeficiency in one of nine genes that promote IFNγ-expression or -effectiveness (*CYBB*, *IFNGR1*, *IFNGR2*, *IL12B*, *IL12RB1*, *IRF8*, *ISG15*, *NEMO* and *STAT1*)[1]. Sequence data from the 1000 Genomes Project further confirm that most individuals inherit two functional *IL12RB1* alleles[66]. However, the same sequence data demonstrate that *IL12RB1* is polymorphic, with multiple SNPs in intronic and exonic regions. Several of these polymorphisms impact *IL12RB1* function and associate with disease susceptibility[3]. For example, T cells complemented with an *IL12RB1* allele containing a collection of linked SNPs termed the “RTR haplotype” (nucleotides C/G/G at chr19 positions 18186618/18180451/18180413) are less responsive to IL12 when compared to T cells complemented with the “QMG haplotype” (nucleotides T/A/C at the same chr19 positions)[46]. The SNPs that comprise the RTR haplotype are associated with tuberculosis

susceptibility in residents of Kyushu Island, Japan[67], cervical adenocarcinoma risk in residents of Seattle, USA[68], breast cancer risk in African American residents of New York City and New Jersey, USA[69], hidradenitis supperativa in Greek Caucasians[70], and leptospirosis susceptibility among residents of Sao Miguel Island, Portugal[71].

Prior to performing our allele-biased expression analysis, we assumed that both alleles of *IL12RB1* were expressed in an immunocompetent individual. However, our data do not support this assumption and instead support the depiction in FIG 7B that, in human lung tissue and T cells, one *IL12RB1* allele is silenced and the other transcriptionally active. This is important, as the allele chosen for expression will likely impact disease susceptibility. Again using the RTR and QMG haplotypes as an example, our sequencing data demonstrate that lung tissue donors N5 and S1 were heterozygotes who both inherited an RTR and QMG haplotype (FIG 1B, Donor N5 and S1 gDNA columns). However, the mRNAs produced in Donor N5 were primarily derived from RTR allele, while the mRNAs produced from Donor S1 were primarily derived from the QMG allele (FIG 1B, Donor N5 and S1 mRNA columns). Based on this information, we would predict the T cells from Donor N5 would respond to IL12 in a similar manner to T cells from someone who is homozygous for the RTR allele (e.g. Donor N1). Likewise, we would also predict that T cells from Donor S1 would respond to IL12 in a similar manner to T cells from someone who is homozygous for the QMG allele (e.g. Donor N4). Our future efforts will test this prediction, as well as determine if other MSMD-associated genes are regulated by monoallelic expression.

Monoallelic expression of autosomal genes is initiated and maintained by a variety of epigenetic mechanisms, including histone modifications, DNA methylation and nuclear organization[18]. The modification of histones can either promote or repress transcription of the associated allele, depending on the nature of the modification. For example, modifications of histone H3 that promote monoallelic expression include dimethylation and trimethylation of Lys4 (H3K4me2, H3K4me3), trimethylation of Lys36 (H3K36me3) and monoacetylation of Lys9 (H3K9ac)[18]. Modifications of histone H3 that repress expression include trimethylation of Lys9 (H3K9me3) and trimethylation of Lys27 (H3K27me3)[18]. Whereas histone modification affects proteins that are proximal to DNA, DNA methylation is a modification of DNA itself (i.e. cytosine) that represses transcription and is the basis for X-chromosome inactivation[72]. An additional epigenetic mechanism is the physical reorganization of all chromatin within the nucleus to permit interchromosomal interactions between an allele and enhancer elements[73]. MicroRNAs have also emerged as mechanism underlying allelic imbalance, as SNPs may create or disrupt microRNA target sites[74–76]. Future studies of *IL12RB1* alleles with an ARF^{mRNA} scores of 100 or 0 (e.g. ch19:18170384, FIG 1B,D) may demonstrate these SNPs to be microRNA binding sites.

Alternative RNA processing introduces variation in T cell responses to the “three signals” that govern T cell function[20] (i.e. Signal 1, antigen recognition; Signal 2, co-stimulation; Signal 3, cytokine stimulation). Once an *IL12RB1* allele is transcribed into a pre-mRNA, T cells must choose whether to alternatively process it (via alternative splicing and polyadenylation) into Isoform 1 or Isoform 2 (FIG 7B). The factors influencing cells’ alternative processing of *IL12RB1* decision include activation status, as primary T cells express Isoform 2 more abundantly than Isoform 1 prior to activation[16]. Our results show

that the exon 9b 3′ splice site and polyA site function efficiently in a minigene setting in the absence of exon 10, which suggests that inclusion of alternative exon 9b is out-competed by splicing from exon 9 to 10. The G-tracts downstream of the *IL12RB1* exon 9b polyA site bind hnRNP H, which regulates pre-mRNA splicing and polyadenylation in a variety of systems[77–79]. hnRNP H is one member of the larger hnRNP family of proteins which facilitate mRNA processing[80]. Although eliminating hnRNP H binding via mutations did not impact T cells choice to express minigene-derived Isoform 1 or Isoform 2, it is possible that hnRNP H regulates the exon 9b polyA site in a manner that is not reflected with our minigenes. Importantly, our studies do not rule out hnRNP H binding as participating in regulation of the endogenous *IL12RB1* gene, since minigene constructs p*B1*[9–11] and p*B1*[9–10] contained portions of *IL12RB1*, rather than the entire gene. Further work is needed to explore this possibility, including testing the hypothesis that hnRNP H knockdown alters T cell *IL12RB1* Iso1:Iso2 ratios, and using hnRNP H RIP-Seq to test if endogenous *IL12RB1* transcripts associate with hnRNP H in T cells (this approach was recently used to identify all hnRNP H bound transcripts in HeLa cells[81]). Additional hnRNPs that function in human T cells include hnRNP L which preferentially binds the pre-mRNA of genes that regulate T cell development[34, 36], and hnRNP LL which facilitates expression of the CD45RO isoform via repression of *PTPRC* exon 4[38, 40, 41].

Should T cells choose to splice the *IL12RB1* pre-mRNA into Isoform 1, the translated protein (IL12Rβ1) will be a type 1 transmembrane protein that localizes to the cell surface and positively regulates human IL12/23 sensitivity by binding the IL12p40-domain common to both cytokines[3]. Given that Isoform 2 lacks the transmembrane domain and has a localization pattern that is distinct from Isoform 1[16, 17], we initially predicted that Isoform 2 would either be non-functional or compete with Isoform 1 for access to IL12. However and unexpectedly, Isoform 2 potentiated IL12 responsiveness in mice and promoted their control of extrapulmonary TB[17]. It was these data that prompted our testing the hypothesis that Iso2 knockdown would attenuate IL12-dependent IFNγ secretion. Our results support this hypothesis and the model depicted in FIG 7C, wherein regardless of which way the *IL12RB1* pre-mRNA is spliced (Isoform 1 or Isoform 2) the resulting protein will promote IL12 responsiveness. What will differ between these isoforms is their biochemical mechanism given Isoform 2′s distinct localization and altered C-terminal amino acid sequence.

In conclusion, we have demonstrated that in primary human lung tissue the *IL12RB1* gene is preferentially expressed from one allele, and that the pre-mRNAs transcribed from *IL12RB1* are processed into either Isoform 1 or Isoform 2 through competition between splicing and alternative polyadenylation of exon 9b. Should T cells choose to splice Isoform 2, our data demonstrate that the resulting protein will function to promote IL12-dependent IFNγ secretion. These results provide a rationale for future investigations of Isoform 2′s biochemical mechanism of action, as well as the epigenetic mechanisms responsible for establishing and sustaining allele-biased expression of *IL12RB1*.

MATERIALS AND METHODS

Human tissues and cell lines

Human lung tissue specimens were provided by the National Disease Research Interchange (NDRI, Philadelphia, PA). Between 1-5 hours postmortem, lung tissue specimens were collected and snap frozen for the NDRI repository. Upon receiving them in our laboratory, specimens were used for nucleic acid extraction and *IL12RB1* amplification. Peripheral blood mononuclear cells (PBMCs) were purified from blood units that were donated by healthy adults, at the Blood Center of Wisconsin (Milwaukee, WI). Donors were excluded if they were taking (or had taken within 2 weeks before collection) any of the following categories of immunosuppressant medications: antineoplastic agent, antiviral agent, corticosteroid (either dermatological or nondermatological), a disease-modifying anti-rheumatic drug, or immunosuppressive mAb drugs. For purifying CD4+ and CD8+ T cells, PBMCs were suspended in a slurry of magnetic bead-Ab conjugates specific to CD4 (clone L200) or CD8 (clone SK1), according to the manufacturer's protocols (BD Biosciences, San Diego, CA). After positive selection and two rounds of washing in PBS, subsets were counted and immediately lysed for RNA and DNA extraction. To determine the extent to which activation influenced allele bias, CD4+ and CD8+ T cells were purified from PBMCs before and after PBMC stimulation with PHA. The Jurkat T cell line was obtained from the American Type Culture Collection (ATCC, Manassas, VA) and passaged per ATCC protocols. BSC40^{Iso2} cells (a BSC40 cell line derivative that stably expresses Isoform 2 mRNA) have been previously described[16]. Cell lines were authenticated by PCR to be mycoplasma-free. All studies using human tissue and cells were approved by the Medical College of Wisconsin (MCW, Milwaukee, WI) Institutional Review Board. Informed consent was obtained from all subjects.

Monoallelic/allele-biased expression analysis

Genomic DNA (gDNA) and messenger RNA (mRNA) were extracted from human tissues and cell lines using the AllPrep DNA/RNA method (Qiagen, Germantown, MD). We performed PCR amplification and Ion Torrent sequencing of *IL12RB1* gDNA/mRNA per our previously reported methods[43]. Single nucleotide polymorphisms (SNPs) in the donor *IL12RB1* gDNA sequence were identified by comparing the donor gDNA sequence to the reference genome build Hg19. Among all the donor and cell line gDNA samples sequenced, we identified eleven positions that were polymorphic (chr19:18170384, 18170755, 18180413, 18180451, 18186575, 18186618, 18188408, 18191664, 18192977, 18194255 and 18197635). Ten of the positions had been previously described and assigned a reference SNP (rs) number (18170384, rs3746190; 18180413, rs401502; 18180451, rs375947; 18186575, rs17852635; 18186618, rs11575934; 18188408, rs11575926; 18191664, rs11086087; 18192977, rs11575925; 18197635, rs436857; 18194255, rs372258967). One of the positions we identified was Jurkat T cell line specific and did not have an assigned rs number (chr19:18170755). Whether a donor or cell line was homozygous or heterozygous for a given SNP was determined by querying the Ion Torrent data to see if only one nucleotide was detected at that site (indicating homozygosity) or two nucleotides were detected at that site (indicating heterozygosity). For donors who were genetically heterozygous at one or more polymorphic sites, the mRNA sequence data from the same

tissue was queried to determine if both *IL12RB1* alleles were equally represented in the mRNA (indicating biallelic expression), or if only one *IL12RB1* allele was preferentially represented in the mRNA (indicating allele-biased expression). We used the allele read frequency (ARF) as a quantitative indicator of the extent to which a specific allele was represented in the gDNA or mRNA reads. The ARF^{gDNA} value of a specific allele is determined by the equation $ARF_P^N = \left(X_P^N / Y_P\right) \times \quad 100$, where X_P^N indicates the number of Ion Torrent reads at gDNA position P that were nucleotide N (either an adenine [A], cytosine [C], guanine [G] or thymine [T]), and Y_P indicates the total number of Ion Torrent reads at position P (all nucleotides). For example, a gDNA $ARF^{A}{}_{18170384}$ value of 50 indicates that 50% of Ion Torrent reads at gDNA position 18170384 were an A, whereas a gDNA $ARF^{A}{}_{18170384}$ value of 100 indicates that 100% of Ion Torrent reads at gDNA position 18170384 were an A. The same equation was used to determine the ARF^{mRNA} value of a specific allele, with the exception that mRNA sequencing information was used for values X_P^N and Y_P. After calculating each allele's ARF^{gDNA} and ARF^{mRNA} values, we could then determine if *IL12RB1* expression was biallelic ($ARF^{mRNA} \cong ARF^{gDNA}$ for both *IL12RB1* alleles) or allele-biased ($ARF^{mRNA} \gg ARF^{gDNA}$ for one *IL12RB1* allele). Per the criteria established by Gendral et al[82], *IL12RB1* expression was considered allele-biased if the predominantly expressed allele was expressed at ≥ 80% and the second allele at ≤ 20%. Our previously reported methods were used to generate and Sanger sequence *IL12RB1* gDNA amplicons and *IL12RB1* cDNA libraries[43].

IL12RB1 minigene construction

Two *IL12RB1* minigenes (p$B1^{9–10}$ and p$B1^{9–11}$) were constructed in anticipation that one or both would recapitulate *IL12RB1* alternative RNA processing. Minigenes and their derivatives (i.e. deletion mutants) were generated using a commercial gene synthesis service (Invitrogen, Carlsbad, CA). p$B1^{9–10}$ was generated by cloning a 2804 bp insert encoding *IL12RB1* exons 9→9b→10 (NCBI Reference Sequence: NG_007366.2, positions 26468-29271) into the HindIII/XbaI site of vector p3xFLAG-CMV7.1 (Sigma-Aldrich). p$B1^{9–11}$ was similarly generated, via cloning into the same site/vector a 3962 bp insert encoding *IL12RB1* exons 9→9b→10→11 (NG_007366.2 positions 26468-30429). Restriction sites were engineered into the minigenes to facilitate generation of deletion mutants. Derivatives of p$B1^{9–10}$ that we generated and used for our study include the minigene ΔpolyA (removal of a 345 bp BsuI-BspEI fragment that encompasses the polyA signal and downstream intron sequence, including the G tracts: the polyadenylation signal in NG_007366.2 is at positions 28232-28237), ΔpolyAΔex10 (removal of a 1190 bp BsuI-HindIII fragment that encompasses the polyA region, downstream intron, and exon 10), Δex9b (removal of a 991 bp HpaI-BspEI fragment that harbors exon 9b, and upstream and downstream intron sequences, including the G tracts), Δex10 (deletion of a 845 bp BspEI-HindIII fragment that removes exon 10 and upstream introns sequences). G-tract mutations were generated by synthesizing a 359 bp BsuI-BspEI fragment (Invitrogen, Carlsbad, CA) spanning the G tract region that contained five GGG to GUG changes (see FIG 5A). Plasmids harboring G tract mutations (p$B1^{9–10}$mutG-tract and p$B1^{9–11}$mutG-tract were made by replacing the wild type fragment with the mutant. For UV cross-linking, an 84 bp

fragment containing the wild type or mutant G tracts was cloned into the EcoRI-HindIII sites of pGEM-3Z (Promega) to generate p3Z-Gtract and p3Zmut.

Minigene transfection and expression analysis

IL12RB1 minigenes were transfected into Jurkat T cells using the Lipofectamine method (Invitrogen). Two days later, mRNA was extracted and used for RT-PCR analysis of minigene-derived Iso1 and Iso2 expression. Specifically, cDNA from minigene transfectants were added to a multiplex PCR reaction comprising three primers: T7 promoter, a forward primer that anneals to a vector-derived sequence upstream of the *IL12RB1* insert (5′-TAATACGACTCACTATAGGG-3′); pcD-myc-r, an outside reverse primer that anneals to a vector-derived sequence downstream of the *IL12RB1* insert (5′-GCTATTCAGATCCTCTTCTG-3′); 9b-Bst, a reverse primer that anneals to an *IL12RB1* exon 9b-derived sequence (5′-CTGGAAGGCGGAGGTTACC-3′). The use of T7 and pcD-myc-r primers ensured that the Iso1 and Iso2 mRNAs we amplified were minigene-derived, and not the endogenous *IL12RB1* isoforms expressed by Jurkat T cells. Amplicons were visualized using standard agarose gel electrophoresis methods.

Semiquantitative PCR

Jurkat cells were transfected with minigenes containing wild type or mutant G-tracts using Lipofectamine 2000 following manufacturer's suggested conditions. Two days later total RNA was isolated using Qiagen RNeasy columns following manufacturer's suggested conditions, followed by reverse transcription. PCR reactions were done using primers described above. Reactions contained alpha-^{32}P dCTP and went 25 cycles, after which products were separated on a 5% non-denaturing acrylamide gel, dried, and quantitated by phosphorimaging. Products were normalized for dCTP content.

UV cross-linking and hnRNP H immunoprecipitation

In vitro transcription (IVT) and hnRNP H immunoprecipitation were performed using previously reported methods[52, 58]. Briefly, 85 nt radiolabeled RNAs that encompass the G tracts were produced using^{32}P-radionucleotides and incubated in HeLa cell nuclear cell extracts known to contain hnRNP H, and RNAs were UV-crosslinked to any associating protein. Cross-linked RNA/protein conjugates were then immunoprecipitated using either anti-hnRNP H antibody or preimmune sera, resolved via SDS-PAGE, and visualized by phosphorimaging.

Design and screen of microRNAs to knockdown Isoform 2 expression

To knockdown Isoform 2 mRNA expression, we designed and expressed five microRNAs targeting *IL12RB1* exon 9b (an mRNA sequence specific to Isoform 2) using the BLOCK-iT Lentiviral Pol II miR RNAi expression system (Invitrogen). The five microRNAs we designed are referred to as miR$^{\pi}$, miR$^{\phi}$, miR$^{\sigma}$, miR$^{\mu}$ and miR^{e}. These five miRs and their sequences are depicted in supplemental FIG S1A; each miR's corresponding target in the *IL12RB1* exon 9b mRNA is depicted in supplemental FIG S1B. The cDNAs encoding each miR were commercially synthesized (Integrated DNA Technologies, Coralville, IA) (supplemental TABLE S1) and cloned into the GFP-miR expression cassette of the

mammalian expression plasmid pcDNA 6.2-GW/EmGFP-miR. GFP-miR containing plasmid clones were identified by colony PCR, Sanger sequenced, and screened for their ability to knockdown Isoform 2 mRNA in BSC40^{Iso2} cells. Specifically, BSC40^{Iso2} cells were transfected with a miR-containing plasmid clone, cultured for two days, and FACS sorted based on GFP expression (supplemental FIG S1C); mRNA from GFP^{+} cells was then used to quantify Isoform 2 mRNA levels per our reported methods[16]. Control BSC40^{Iso2} cells were transfected with a miR that does not target any human gene (miR^{Neg}, the cDNA sequence for which was provided by Invitrogen and is also reported in supplemental TABLE S1). Among the five miRs we designed and generated, only two miRs (miR$^{\sigma}$ and miR$^{\mu}$) caused a ≥90% reduction in Isoform 2 mRNA levels relative to miR^{Neg} controls (supplemental FIG S1D); the three other miRs (miR$^{\pi}$, miR$^{\phi}$, and miR^{e}) were unable to knockdown Isoform 2 mRNA (data not shown). We then moved forward and cloned the GFP-miR$^{\sigma}$, GFP-miR$^{\mu}$ and GFP-miR^{Neg} expression cassettes into lentiviral vector pLenti6. Lentivirus stocks were generated, titered and stored at -80°C.

Lentiviral Transduction

Jurkat cell cultures were maintained in complete RPMI (cRPMI) and transduced with GFP-miR containing pLenti6 lentivirus per the methods of Denning et al[83]. Transduced cells were then cultured for one week in selection media (cRPMI with 10 μg/mL blasticidin) and FACS sorted based on GFP expression. To reduce intra- and inter-experiment variation, separate cultures were transduced with each miR on the same day, and FACS sorted on the same day. In this manner, Jurkat cells expressing either miR$^{\sigma}$, miR$^{\mu}$ or miR^{Neg} were purified.

IL12-stimulation assay

Purified Jurkat cells expressing miR$^{\sigma}$, miR$^{\mu}$ or miR^{Neg} were stimulated in cRPMI containing either 1 μg/mL phytohemagglutinin (PHA alone), PHA and 1 ng/mL recombinant human IL12 (PHA+IL12^{Lo}), or PHA and 10 ng/mL recombinant human IL12 (PHA+IL12^{Hi}). Recombinant human IL12 was purchased from R&D Systems (Minneapolis, MN). Two days after stimulation, cells and their supernatants were collected and separated; the cells were counted and lysed for RT-PCR analysis, while the supernatants were frozen and later used for ELISA analysis.

RT-PCR analysis of transduced Jurkat cells

RNA from miR-transduced, stimulated Jurkat cells was collected and used for RT-PCR analysis of Isoform 1, Isoform 2, IFNγ and GAPDH mRNA levels. Isoform 1 and Isoform 2 mRNA levels were visualized using our previously reported multiplex PCR method[16]. The level of Isoform 1 mRNA in miR-transductants was also assessed quantitatively using our previously reported SYBR green PCR method[16]. Notably, the same SYBR green method could not reliably measure Isoform 2 mRNA levels in miR-transductants, and instead produced aberrant amplicons (data not shown) that were possibly due to interference from Iso2 specific miRs present in the RNA preparation. It was for this reason we used conventional PCR and agarose gel electrophoresis to visualize Isoform 2 mRNA levels in miR-transductants. The mRNA levels of IFNγ and GAPDH were determined using TaqMan Gene Expression Assays (Applied Biosystems, Foster City, CA), using the primer/probe sets Hs00989291_m1 (IFNγ) and Hs99999905_m1 (GAPDH), and the C_T for each gene

determined using an iQ5 Real-Time PCR System (BioRad, Hercules, CA). For each biological replicate, the ΔC_T was determined ($C_T^{IFN\gamma}$- C_T^{GAPDH}) and the IFNγ mRNA level (x) calculated using the equation $x = 2^{-\Delta CT}$.

ELISA analysis

Supernatants from miR-transduced, stimulated Jurkat cells were used for ELISA analysis of secreted IFNγ levels. The concentration of human IFNγ in each supernatant was determined using the OptEIA system (BD Biosciences, San Jose, CA). For graphing and statistical analysis, IFNγ concentrations were normalized to the number of Jurkat cells present in each well.

Graphing and statistical analysis

Graphs were prepared using Graph Pad Prism version 5.0. Statistical analyses were performed using the bundled software of Prism. Standard power formulas were used to calculate sample size and ensure adequate power to detect statistical differences. Statistical differences between two groups were determined using Student's t-test, while differences between three or more groups were determined using one-way ANOVA; the variance was similar between groups that were statistically compared. Differences were considered significant if $p < 0.05$, and is graphically indicated by an asterisk.

Supplementary Material

Refer to Web version on PubMed Central for supplementary material.

Acknowledgments

We would like to thank and acknowledge the following individuals, whose work contributed to indicated Figures: Jill Waukau and Christine Bengtson (Figures 1 and 2), Mark McNally and Lisa McNally (Figures 4 and 5), Katrina Monson and Brady Brooks (Figure 6). We would also like to thank Abigail Robinson for the chromosome 19 karyotype image in Figure 7. This work was supported by the Medical College of Wisconsin (MCW) and National Institutes of Health grant R01 AI121212 (to R.T.R.).

References

1. Bustamante J, Boisson-Dupuis S, Abel L, Casanova JL. Mendelian susceptibility to mycobacterial disease: genetic, immunological, and clinical features of inborn errors of IFN-gamma immunity. Semin Immunol. 2014; 26(6):454–70. [PubMed: 25453225]
2. de Beaucoudrey L, Samarina A, Bustamante J, Cobat A, Boisson-Dupuis S, Feinberg J, et al. Revisiting human IL-12Rbeta1 deficiency: a survey of 141 patients from 30 countries. Medicine (Baltimore). 2010; 89(6):381–402. [PubMed: 21057261]
3. Robinson RT. IL12Rbeta1: the cytokine receptor that we used to know. Cytokine. 2015; 71(2):348–59. [PubMed: 25516297]
4. van de Vosse E, Haverkamp MH, Ramirez-Alejo N, Martinez-Gallo M, Blancas-Galicia L, Metin A, et al. IL-12Rbeta1 deficiency: mutation update and description of the IL12RB1 variation database. Hum Mutat. 2013; 34(10):1329–39. [PubMed: 23864330]
5. Dhiman N, Ovsyannikova IG, Cunningham JM, Vierkant RA, Kennedy RB, Pankratz VS, et al. Associations between measles vaccine immunity and single-nucleotide polymorphisms in cytokine and cytokine receptor genes. J Infect Dis. 2007; 195(1):21–9. [PubMed: 17152005]
6. White SJ, Haralambieva IH, Ovsyannikova IG, Vierkant RA, O'Byrne MM, Poland GA. Replication of associations between cytokine and cytokine receptor single nucleotide polymorphisms and

measles-specific adaptive immunophenotypic extremes. Hum Immunol. 2012; 73(6):636–40. [PubMed: 22504412]

7. Li X, Hawkins GA, Ampleford EJ, Moore WC, Li H, Hastie AT, et al. Genome-wide association study identifies TH1 pathway genes associated with lung function in asthmatic patients. J Allergy Clin Immunol. 2013; 132(2):313–20 e15. [PubMed: 23541324]
8. Takahashi N, Akahoshi M, Matsuda A, Ebe K, Inomata N, Obara K, et al. Association of the IL12RB1 promoter polymorphisms with increased risk of atopic dermatitis and other allergic phenotypes. Hum Mol Genet. 2005; 14(21):3149–59. [PubMed: 16159888]
9. Hong X, Wang G, Liu X, Kumar R, Tsai HJ, Arguelles L, et al. Gene polymorphisms, breast-feeding, and development of food sensitization in early childhood. J Allergy Clin Immunol. 2011; 128(2):374–81 e2. [PubMed: 21689850]
10. Oppmann B, Lesley R, Blom B, Timans JC, Xu Y, Hunte B, et al. Novel p19 protein engages IL-12p40 to form a cytokine, IL-23, with biological activities similar as well as distinct from IL-12. Immunity. 2000; 13(5):715–25. [PubMed: 11114383]
11. Presky DH, Yang H, Minetti LJ, Chua AO, Nabavi N, Wu CY, et al. A functional interleukin 12 receptor complex is composed of two beta-type cytokine receptor subunits. Proc Natl Acad Sci U S A. 1996; 93(24):14002–7. [PubMed: 8943050]
12. Parham C, Chirica M, Timans J, Vaisberg E, Travis M, Cheung J, et al. A receptor for the heterodimeric cytokine IL-23 is composed of IL-12Rbeta1 and a novel cytokine receptor subunit, IL-23R. J Immunol. 2002; 168(11):5699–708. [PubMed: 12023369]
13. Khader SA, Pearl JE, Sakamoto K, Gilmartin L, Bell GK, Jelley-Gibbs DM, et al. IL-23 compensates for the absence of IL-12p70 and is essential for the IL-17 response during tuberculosis but is dispensable for protection and antigen-specific IFN-gamma responses if IL-12p70 is available. J Immunol. 2005; 175(2):788–95. [PubMed: 16002675]
14. Cooper AM, Dalton DK, Stewart TA, Griffin JP, Russell DG, Orme IM. Disseminated tuberculosis in interferon gamma gene-disrupted mice. J Exp Med. 1993; 178(6):2243–7. [PubMed: 8245795]
15. Flynn JL, Chan J, Triebold KJ, Dalton DK, Stewart TA, Bloom BR. An essential role for interferon gamma in resistance to Mycobacterium tuberculosis infection. J Exp Med. 1993; 178(6):2249–54. [PubMed: 7504064]
16. Ford NR, Miller HE, Reeme AE, Waukau J, Bengtson C, Routes JM, et al. Inflammatory signals direct expression of human IL12RB1 into multiple distinct isoforms. J Immunol. 2012; 189(9): 4684–94. [PubMed: 23024274]
17. Ray AA, Fountain JJ, Miller HE, Cooper AM, Robinson RT. IL12Rbeta1DeltaTM is a secreted product of il12rb1 that promotes control of extrapulmonary tuberculosis. Infect Immun. 2015; 83(2):560–71. [PubMed: 25404030]
18. Reinius B, Sandberg R. Random monoallelic expression of autosomal genes: stochastic transcription and allele-level regulation. Nat Rev Genet. 2015; 16(11):653–64. [PubMed: 26442639]
19. Chang X. RNA-binding protein hnRNPLL as a critical regulator of lymphocyte homeostasis and differentiation. Wiley Interdiscip Rev RNA. 2016; 7(3):295–302. [PubMed: 26821996]
20. Martinez NM, Lynch KW. Control of alternative splicing in immune responses: many regulators, many predictions, much still to learn. Immunol Rev. 2013; 253(1):216–36. [PubMed: 23550649]
21. Ku CJ, Lim KC, Kalantry S, Maillard I, Engel JD, Hosoya T. A monoallelic-to-biallelic T-cell transcriptional switch regulates GATA3 abundance. Genes Dev. 2015; 29(18):1930–41. [PubMed: 26385963]
22. Brady BL, Steinel NC, Bassing CH. Antigen receptor allelic exclusion: an update and reappraisal. J Immunol. 2010; 185(7):3801–8. [PubMed: 20858891]
23. Bayley JP, van Rietschoten JG, Bakker AM, van Baarsen L, Kaijzel EL, Wierenga EA, et al. Allele-specific expression of the IL-1 alpha gene in human CD4+ T cell clones. J Immunol. 2003; 171(5):2349–53. [PubMed: 12928381]
24. Bix M, Locksley RM. Independent and epigenetic regulation of the interleukin-4 alleles in CD4+ T cells. Science. 1998; 281(5381):1352–4. [PubMed: 9721100]
25. Calado DP, Paixao T, Holmberg D, Haury M. Stochastic monoallelic expression of IL-10 in T cells. J Immunol. 2006; 177(8):5358–64. [PubMed: 17015721]

26. Hollander GA, Zuklys S, Morel C, Mizoguchi E, Mobisson K, Simpson S, et al. Monoallelic expression of the interleukin-2 locus. Science. 1998; 279(5359):2118–21. [PubMed: 9516115]
27. Kelly BL, Locksley RM. Coordinate regulation of the IL-4, IL-13, and IL-5 cytokine cluster in Th2 clones revealed by allelic expression patterns. J Immunol. 2000; 165(6):2982–6. [PubMed: 10975806]
28. Rhoades KL, Singh N, Simon I, Glidden B, Cedar H, Chess A. Allele-specific expression patterns of interleukin-2 and Pax-5 revealed by a sensitive single-cell RT-PCR analysis. Curr Biol. 2000; 10(13):789–92. [PubMed: 10898982]
29. Riviere I, Sunshine MJ, Littman DR. Regulation of IL-4 expression by activation of individual alleles. Immunity. 1998; 9(2):217–28. [PubMed: 9729042]
30. van Rietschoten JG, Verzijlbergen KF, Gringhuis SI, van der Pouw Kraan TC, Bayley JP, Wierenga EA, et al. Differentially methylated alleles in a distinct region of the human interleukin-1alpha promoter are associated with allele-specific expression of IL-1alpha in CD4+ T cells. Blood. 2006; 108(7):2143–9. [PubMed: 16788102]
31. Chaudhury A, Chander P, Howe PH. Heterogeneous nuclear ribonucleoproteins (hnRNPs) in cellular processes: Focus on hnRNP E1's multifunctional regulatory roles. RNA. 2010; 16(8): 1449–62. [PubMed: 20584894]
32. Yeh YM, Chen CY, Huang PR, Hsu CW, Wu CC, Wang TC. Proteomic analyses of genes regulated by heterogeneous nuclear ribonucleoproteins A/B in Jurkat cells. Proteomics. 2014; 14(11):1357–66. [PubMed: 24634410]
33. Veraldi KL, Arhin GK, Martincic K, Chung-Ganster LH, Wilusz J, Milcarek C. hnRNP F influences binding of a 64-kilodalton subunit of cleavage stimulation factor to mRNA precursors in mouse B cells. Mol Cell Biol. 2001; 21(4):1228–38. [PubMed: 11158309]
34. Gaudreau MC, Heyd F, Bastien R, Wilhelm B, Moroy T. Alternative splicing controlled by heterogeneous nuclear ribonucleoprotein L regulates development, proliferation, and migration of thymic pre-T cells. J Immunol. 2012; 188(11):5377–88. [PubMed: 22523384]
35. Rothrock CR, House AE, Lynch KW. HnRNP L represses exon splicing via a regulated exonic splicing silencer. EMBO J. 2005; 24(15):2792–802. [PubMed: 16001081]
36. Shankarling G, Cole BS, Mallory MJ, Lynch KW. Transcriptome-wide RNA interaction profiling reveals physical and functional targets of hnRNP L in human T cells. Mol Cell Biol. 2014; 34(1): 71–83. [PubMed: 24164894]
37. Tong A, Nguyen J, Lynch KW. Differential expression of CD45 isoforms is controlled by the combined activity of basal and inducible splicing-regulatory elements in each of the variable exons. J Biol Chem. 2005; 280(46):38297–304. [PubMed: 16172127]
38. Topp JD, Jackson J, Melton AA, Lynch KW. A cell-based screen for splicing regulators identifies hnRNP LL as a distinct signal-induced repressor of CD45 variable exon 4. RNA. 2008; 14(10): 2038–49. [PubMed: 18719244]
39. Chang X, Li B, Rao A. RNA-binding protein hnRNPLL regulates mRNA splicing and stability during B-cell to plasma-cell differentiation. Proc Natl Acad Sci U S A. 2015; 112(15):E1888–97. [PubMed: 25825742]
40. Oberdoerffer S, Moita LF, Neems D, Freitas RP, Hacohen N, Rao A. Regulation of CD45 alternative splicing by heterogeneous ribonucleoprotein, hnRNPLL. Science. 2008; 321(5889): 686–91. [PubMed: 18669861]
41. Wu Z, Jia X, de la Cruz L, Su XC, Marzolf B, Troisch P, et al. Memory T cell RNA rearrangement programmed by heterogeneous nuclear ribonucleoprotein hnRNPLL. Immunity. 2008; 29(6):863–75. [PubMed: 19100700]
42. Meininger I, Griesbach RA, Hu D, Gehring T, Seeholzer T, Bertossi A, et al. Alternative splicing of MALT1 controls signalling and activation of CD4(+) T cells. Nat Commun. 2016; 7:11292. [PubMed: 27068814]
43. Turner AJ, Aggarwal P, Miller HE, Waukau J, Routes JM, Broeckel U, et al. The introduction of RNA-DNA differences underlies interindividual variation in the human IL12RB1 mRNA repertoire. Proc Natl Acad Sci U S A. 2015; 112(50):15414–9. [PubMed: 26621740]

44. Miller HE, Robinson RT. Early control of Mycobacterium tuberculosis infection requires il12rb1 expression by rag1-dependent lineages. Infect Immun. 2012; 80(11):3828–41. [PubMed: 22907814]
45. Xiao Z, Casey KA, Jameson SC, Curtsinger JM, Mescher MF. Programming for CD8 T cell memory development requires IL-12 or type I IFN. J Immunol. 2009; 182(5):2786–94. [PubMed: 19234173]
46. van de Vosse E, de Paus RA, van Dissel JT, Ottenhoff TH. Molecular complementation of IL-12Rbeta1 deficiency reveals functional differences between IL-12Rbeta1 alleles including partial IL-12Rbeta1 deficiency. Hum Mol Genet. 2005; 14(24):3847–55. [PubMed: 16293671]
47. Abraham RT, Weiss A. Jurkat T cells and development of the T-cell receptor signalling paradigm. Nat Rev Immunol. 2004; 4(4):301–8. [PubMed: 15057788]
48. Lou H, Cote GJ, Gagel RF. The calcitonin exon and its flanking intronic sequences are sufficient for the regulation of human calcitonin/calcitonin gene-related peptide alternative RNA splicing. Mol Endocrinol. 1994; 8(12):1618–26. [PubMed: 7535892]
49. Lou H, Gagel RF. Alternative RNA processing–its role in regulating expression of calcitonin/calcitonin gene-related peptide. J Endocrinol. 1998; 156(3):401–5. [PubMed: 9582495]
50. Millevoi S, Vagner S. Molecular mechanisms of eukaryotic pre-mRNA 3' end processing regulation. Nucleic Acids Res. 2010; 38(9):2757–74. [PubMed: 20044349]
51. Caputi M, Zahler AM. Determination of the RNA binding specificity of the heterogeneous nuclear ribonucleoprotein (hnRNP) H/H'/F/2H9 family. J Biol Chem. 2001; 276(47):43850–9. [PubMed: 11571276]
52. Fogel BL, McNally MT. A cellular protein, hnRNP H, binds to the negative regulator of splicing element from Rous sarcoma virus. J Biol Chem. 2000; 275(41):32371–8. [PubMed: 10934202]
53. Hastings ML, Wilson CM, Munroe SH. A purine-rich intronic element enhances alternative splicing of thyroid hormone receptor mRNA. RNA. 2001; 7(6):859–74. [PubMed: 11421362]
54. Kralovicova J, Vorechovsky I. Position-dependent repression and promotion of DQB1 intron 3 splicing by GGGG motifs. J Immunol. 2006; 176(4):2381–8. [PubMed: 16455996]
55. Marcucci R, Baralle FE, Romano M. Complex splicing control of the human Thrombopoietin gene by intronic G runs. Nucleic Acids Res. 2007; 35(1):132–42. [PubMed: 17158158]
56. Mauger DM, Lin C, Garcia-Blanco MA. hnRNP H and hnRNP F complex with Fox2 to silence fibroblast growth factor receptor 2 exon IIIc. Mol Cell Biol. 2008; 28(17):5403–19. [PubMed: 18573884]
57. McCullough AJ, Berget SM. G triplets located throughout a class of small vertebrate introns enforce intron borders and regulate splice site selection. Mol Cell Biol. 1997; 17(8):4562–71. [PubMed: 9234714]
58. McNally LM, Yee L, McNally MT. Heterogeneous nuclear ribonucleoprotein H is required for optimal U11 small nuclear ribonucleoprotein binding to a retroviral RNA-processing control element: implications for U12-dependent RNA splicing. J Biol Chem. 2006; 281(5):2478–88. [PubMed: 16308319]
59. Yeo G, Hoon S, Venkatesh B, Burge CB. Variation in sequence and organization of splicing regulatory elements in vertebrate genes. Proc Natl Acad Sci U S A. 2004; 101(44):15700–5. [PubMed: 15505203]
60. Dominguez C, Allain FH. NMR structure of the three quasi RNA recognition motifs (qRRMs) of human hnRNP F and interaction studies with Bcl-x G-tract RNA: a novel mode of RNA recognition. Nucleic Acids Res. 2006; 34(13):3634–45. [PubMed: 16885237]
61. Fieschi C, Dupuis S, Catherinot E, Feinberg J, Bustamante J, Breiman A, et al. Low penetrance, broad resistance, and favorable outcome of interleukin 12 receptor beta1 deficiency: medical and immunological implications. J Exp Med. 2003; 197(4):527–35. [PubMed: 12591909]
62. Chua AO, Wilkinson VL, Presky DH, Gubler U. Cloning and characterization of a mouse IL-12 receptor-beta component. J Immunol. 1995; 155(9):4286–94. [PubMed: 7594587]
63. Robinson RT, Khader SA, Martino CA, Fountain JJ, Teixeira-Coelho M, Pearl JE, et al. Mycobacterium tuberculosis infection induces il12rb1 splicing to generate a novel IL-12Rbeta1 isoform that enhances DC migration. J Exp Med. 2010; 207(3):591–605. [PubMed: 20212068]

64. Showe LC, Wysocka M, Wang B, Lineman-Williams D, Peritt D, Showe MK, et al. Structure of the mouse IL-12R beta 1 chain and regulation of its expression in BCG/LPS-treated mice. Ann N Y Acad Sci. 1996; 795:413–5. [PubMed: 8958970]

65. Yamamoto K, Kobayashi H, Miura O, Hirosawa S, Miyasaka N. Assignment of IL12RB1 and IL12RB2, interleukin-12 receptor beta 1 and beta 2 chains, to human chromosome 19 band p13.1 and chromosome 1 band p31.2, respectively, by in situ hybridization. Cytogenet Cell Genet. 1997; 77(3–4):257–8. [PubMed: 9284929]

66. Genomes Project C, Abecasis GR, Auton A, Brooks LD, DePristo MA, Durbin RM, et al. An integrated map of genetic variation from 1,092 human genomes. Nature. 2012; 491(7422):56–65. [PubMed: 23128226]

67. Akahoshi M, Nakashima H, Miyake K, Inoue Y, Shimizu S, Tanaka Y, et al. Influence of interleukin-12 receptor beta1 polymorphisms on tuberculosis. Hum Genet. 2003; 112(3):237–43. [PubMed: 12596048]

68. Hussain SK, Madeleine MM, Johnson LG, Du Q, Galloway DA, Daling JR, et al. Nucleotide variation in IL-10 and IL-12 and their receptors and cervical and vulvar cancer risk: a hybrid case-parent triad and case-control study. Int J Cancer. 2013; 133(1):201–13. [PubMed: 23280621]

69. Quan L, Gong Z, Yao S, Bandera EV, Zirpoli G, Hwang H, et al. Cytokine and cytokine receptor genes of the adaptive immune response are differentially associated with breast cancer risk in American women of African and European ancestry. Int J Cancer. 2014; 134(6):1408–21. [PubMed: 23996684]

70. Giatrakos S, Huse K, Kanni T, Tzanetakou V, Kramer M, Grech I, et al. Haplotypes of IL-12Rbeta1 impact on the clinical phenotype of hidradenitis suppurativa. Cytokine. 2013; 62(2): 297–301. [PubMed: 23557799]

71. Esteves LM, Bulhoes SM, Branco CC, Mota FM, Paiva C, Cabral R, et al. Human leptospirosis: seroreactivity and genetic susceptibility in the population of Sao Miguel Island (Azores, Portugal). PLoS One. 2014; 9(9):e108534. [PubMed: 25255143]

72. Ruhrmann S, Stridh P, Kular L, Jagodic M. Genomic imprinting: A missing piece of the Multiple Sclerosis puzzle. Int J Biochem Cell Biol. 2015; 67:49–57. [PubMed: 26002250]

73. Monahan K, Lomvardas S. Monoallelic expression of olfactory receptors. Annu Rev Cell Dev Biol. 2015; 31:721–40. [PubMed: 26359778]

74. Kim J, Bartel DP. Allelic imbalance sequencing reveals that single-nucleotide polymorphisms frequently alter microRNA-directed repression. Nat Biotechnol. 2009; 27(5):472–7. [PubMed: 19396161]

75. Miller CL, Haas U, Diaz R, Leeper NJ, Kundu RK, Patlolla B, et al. Coronary heart disease-associated variation in TCF21 disrupts a miR-224 binding site and miRNA-mediated regulation. PLoS Genet. 2014; 10(3):e1004263. [PubMed: 24676100]

76. Nicoloso MS, Sun H, Spizzo R, Kim H, Wickramasinghe P, Shimizu M, et al. Single-nucleotide polymorphisms inside microRNA target sites influence tumor susceptibility. Cancer Res. 2010; 70(7):2789–98. [PubMed: 20332227]

77. Gautrey H, Jackson C, Dittrich AL, Browell D, Lennard T, Tyson-Capper A. SRSF3 and hnRNP H1 regulate a splicing hotspot of HER2 in breast cancer cells. RNA Biol. 2015; 12(10):1139–51. [PubMed: 26367347]

78. Lee YB, Chen HJ, Peres JN, Gomez-Deza J, Attig J, Stalekar M, et al. Hexanucleotide repeats in ALS/FTD form length-dependent RNA foci, sequester RNA binding proteins, and are neurotoxic. Cell Rep. 2013; 5(5):1178–86. [PubMed: 24290757]

79. McNally MT. RNA processing control in avian retroviruses. Front Biosci. 2008; 13:3869–83. [PubMed: 18508481]

80. Geuens T, Bouhy D, Timmerman V. The hnRNP family: insights into their role in health and disease. Hum Genet. 2016; 135(8):851–67. [PubMed: 27215579]

81. Uren PJ, Bahrami-Samani E, de Araujo PR, Vogel C, Qiao M, Burns SC, et al. High-throughput analyses of hnRNP H1 dissects its multi-functional aspect. RNA Biol. 2016; 13(4):400–11. [PubMed: 26760575]

82. Gendrel AV, Attia M, Chen CJ, Diabangouaya P, Servant N, Barillot E, et al. Developmental dynamics and disease potential of random monoallelic gene expression. Dev Cell. 2014; 28(4): 366–80. [PubMed: 24576422]

83. Denning W, Das S, Guo S, Xu J, Kappes JC, Hel Z. Optimization of the transductional efficiency of lentiviral vectors: effect of sera and polycations. Mol Biotechnol. 2013; 53(3):308–14. [PubMed: 22407723]

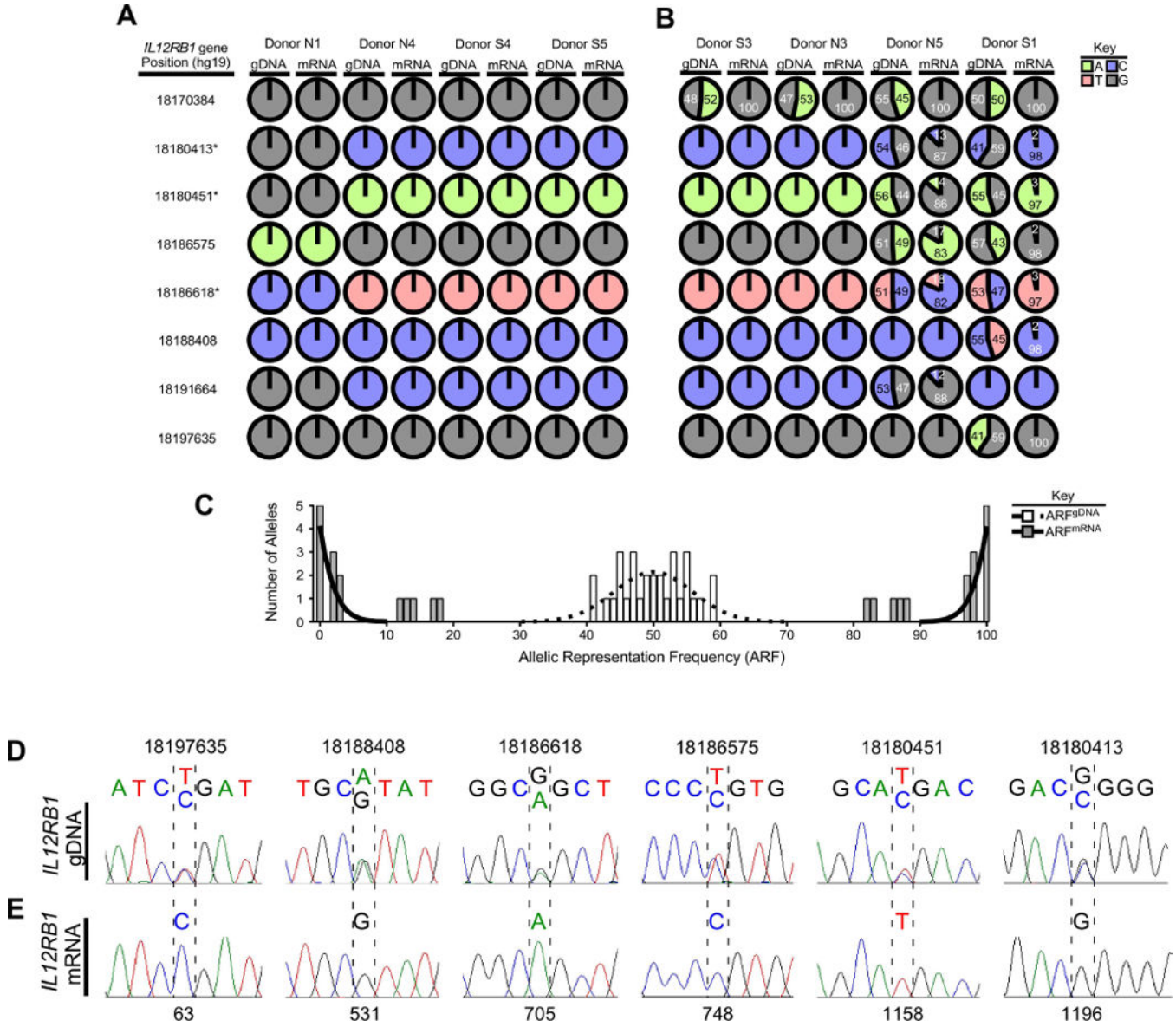

FIGURE 1.

IL12RB1 expression in human lung tissue is allele-biased. **(A-C)** *IL12RB1* gDNA and mRNA from 8 lung tissue donors (N1, N4, S4, S5, S3, N3, N5, S1) was sequenced via Ion Torrent. For each donor, the *IL12RB1* gDNA sequence was queried at 11 polymorphic sites (18170384, 18170755, 18180413, 18180451, 18186575, 18186618, 18188408, 18191664, 18192977, 18194255 and 18197635) to determine if they were homozygous (i.e. only 1 nt was read at that site) or heterozygous (i.e. 2 nts were read at that site). The data from each donor are represented by pie charts indicating the nts detected at each site (G, gray; T, red; A, green; C, blue) and their relative representation among all reads of that site. We similarly queried and analyzed *IL12RB1* mRNA sequence data from the same tissue specimens. Shown are **(A)** *IL12RB1* gDNA and mRNA sequence data from four donors (N1, N4, S4 and S5) who were homozygous at all 11 polymorphic sites, as well as **(B-C)** *IL12RB1* gDNA and mRNA sequence data from four donors (S3, N3, N5 and S1) who were

heterozygous at ≥1 polymorphic sites. The numbers in each chart indicate the frequency with which the indicated allele was represented among all reads of that site (i.e. the allele read frequency, or ARF). The asterisks next to *IL12RB1* gene positions 18186618/18180451/18180413 indicate the linked SNPs that comprise the "RTR haplotype" and "QMG haplotype"[4, 46]. **(C)** A histogram depicting the distribution of gDNA ARF values of each heterozygous allele (open bars), and the mRNA ARF values of the same alleles (closed bars). Nonlinear regression analysis was used to test the Gaussian distribution of the gDNA ARF values, and is depicted by a dotted regression line (r^2=0.7, mean=50.0); mRNA ARF values were bifurcated and non-Gaussian (solid regression line). **(D)** Donor S1 lung gDNA was amplified with primers flanking 6 polymorphic sites in the *IL12RB1* gene (18180413, 18180451, 18186575, 18186618, 18188408, and 18197635); amplicons were Sanger sequenced. Shown are representative Sanger traces demonstrating 2 nts at gDNA positions 18197635 (T/C), 18188408 (A/G), 18186618 (G/A), 18186575 (T/C), 18180451 (T/C), and 18180413 (G/C). **(E)** mRNA from the same specimen was used to make an *IL12RB1* cDNA library, of which 10 clones were randomly chosen for Sanger sequencing. Shown are the Sanger traces of regions that correspond to nts transcribed from the gDNA alleles shown in **(D)**. Indicated by hatched lines are the cDNA nt positions (63, 531, 705, 748, 1158 and 1196) that correspond to the above polymorphic gDNA positions. In contrast to the gDNA traces, there is only 1 nt present at each cDNA position, representing the gDNA allele from which that mRNA was originally transcribed. All 10 cDNA clones contained the same nt at positions 63 (C), 531 (G), 705 (A), 748 (C), 1158 (T) and 1196 (G).

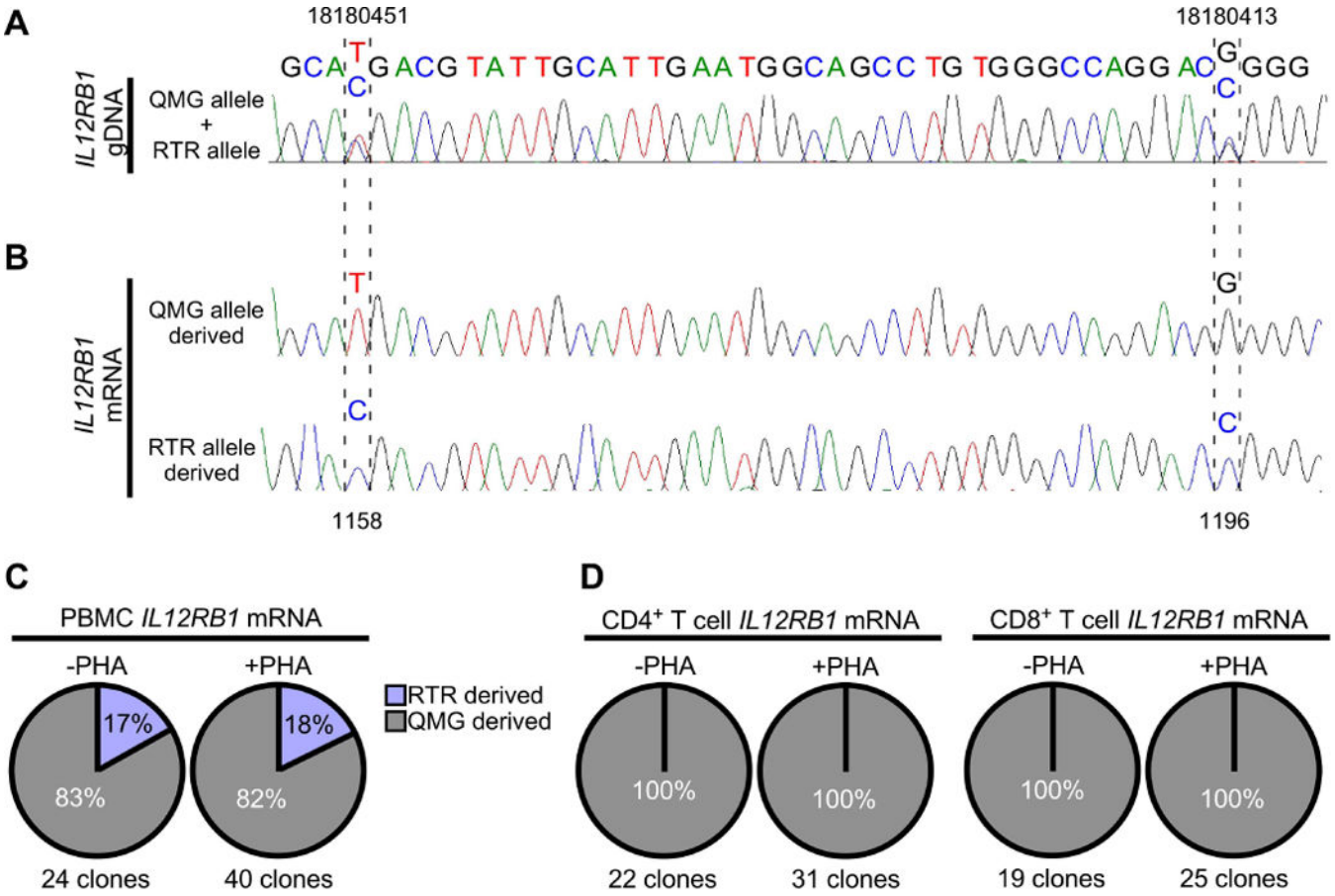

FIGURE 2.

Allele-biased *IL12RB1* expression in human PBMCs and T cells. PBMCs were isolated from 9 healthy adults; one PBMC portion was immediately lysed for gDNA/mRNA extraction, while the other portion was cultured with stimulant (PHA) prior to gDNA/mRNA extraction. PBMCs from 3 donors were further used to isolate $CD4^+$ and $CD8^+$ T cells, before (-PHA) and after PBMC stimulation (+PHA). PBMC gDNA was amplified with primers flanking 2 polymorphic sites in *IL12RB1* exon 10 (18180451 and 18180413) that are constituents of the QMG allele (18180451T and 18180413G) or RTR allele (18180451C and 18180413C). Shown in **(A)** is the Sanger trace of a donor who was heterozygous for the QMG and RTR alleles, as indicated by 2 nts at gDNA positions 18180451 (T/C), and 18180413 (G/C). **(B)** mRNA from the same PBMC and T cell preparations (-PHA and +PHA) was used to generate donor- and cell-specific *IL12RB1* cDNA libraries. From each library, multiple cDNA clones were randomly selected for Sanger sequencing. Shown are representative Sanger traces of clones transcribed from the QMG allele (top) and RTR allele (bottom); in contrast to the gDNA traces, there is only 1 nt present at each cDNA position, representing the gDNA allele from which that mRNA was originally transcribed. Indicated by hatched lines are the 2 cDNA positions (1158 and 1196) that correspond to nts transcribed from the gDNA SNPs above (18180451 and 18180413, respectively). **(C-D)** Pie charts depicting the relative representation QMG-derived cDNA clones (gray) and RTR-derived cDNA clones (blue) in **(C)** -PHA and +PHA PBMC preparations, and **(D)** -PHA and

+PHA T cell preparations. Percentages are taken from the pooled Sanger sequencing data of all donors. The total number of clone sequences analyzed in this manner is indicated below each chart.

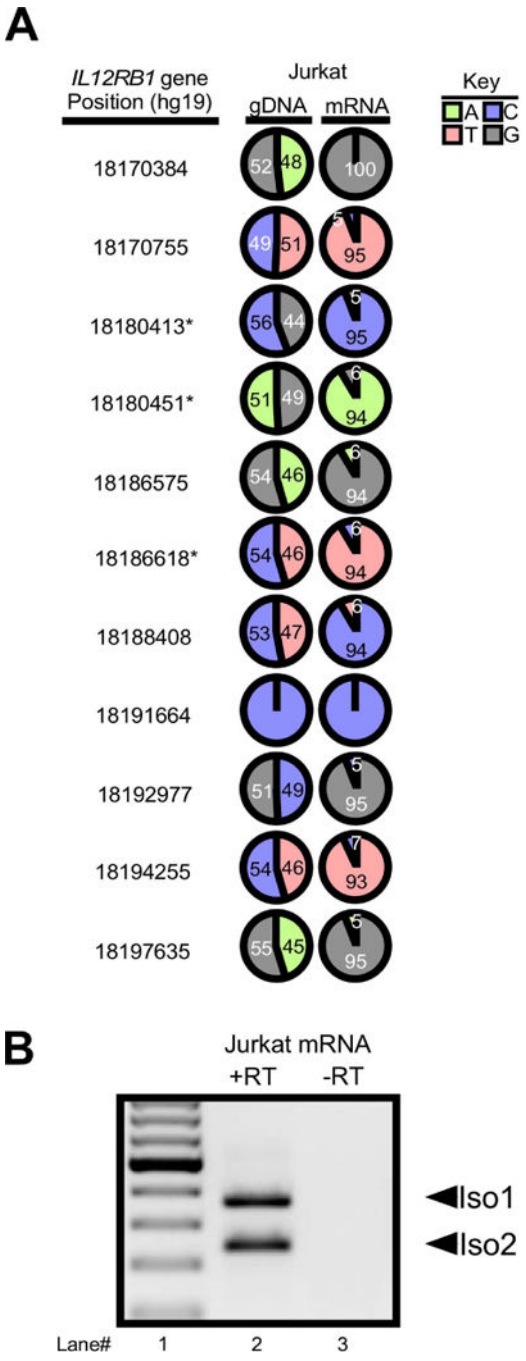

FIGURE 3.

IL12RB1 expression in the Jurkat T cell line is allele-biased and results in the production of Isoform 1 and Isoform 2. **(A)** Jurkat cell *IL12RB1* gDNA and mRNA were sequenced and analyzed in manner identical to that described in FIG 1A–C. The results demonstrate that Jurkat cells are polymorphic at 9 gDNA positions (18170384, 18170755, 18180413, 18180451, 18186575, 18186618, 18188408, 18194255 and 18197635); like primary human tissue, the range of ARF^{gDNA} values for these 9 positions was consistent with equal allelic representation (44%-56%), while the ARF^{mRNA} values were biased towards one allele

(95%-100%) at the expense of the other allele (0-5%). **(B)** Jurkat mRNA was converted to cDNA, which was then used for Isoform 1 and Isoform 2 PCR amplification. Shown are the electrophoresis patterns of (lane *1*) a ladder control and (*lane 2*) Jurkat T cell cDNA amplicons; (*lane 3*) a “no RT control” was also amplified to confirm cDNA specificity.

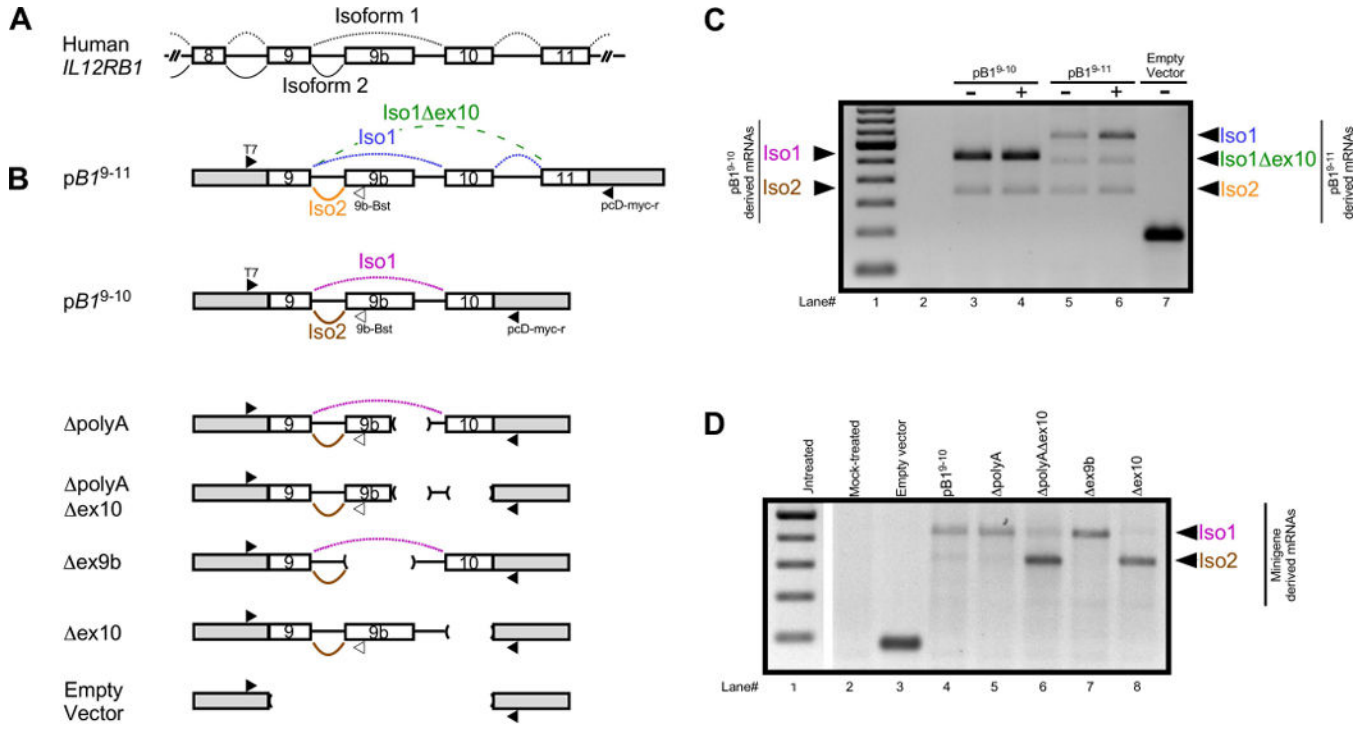

FIGURE 4.

Minigene analysis of *IL12RB1* alternative RNA processing. (**A**) Human *IL12RB1* and the splicing patterns that result in expression of Isoform 1 (black dotted line) and Isoform 2 (black solid line). (**B**) The *IL12RB1* minigenes that were used in our study, with the vector backbone represented by gray boxes at the 5′ and 3′ ends, the exons by open boxes, and the introns by solid lines between boxes. The minigene p*B1*$^{9–11}$ contained *IL12RB1* exons 9, 9b, 10 and 11, as well as their intervening introns. Shown alongside the minigene are annealing sites of the 3 primers (T7, pcD-myc-r, and 9b-Bst) that were used for multiplex amplification of p*B1*$^{9–11}$-derived Iso1 mRNA (the splicing pattern of which is shown by the blue dotted line), p*B1*$^{9–11}$-derived Iso2 mRNA (orange solid line), and a p*B1*$^{9–11}$-derived minor variant (Iso1Δex10, green dashed line). The minigene p*B1*$^{9–10}$ contained *IL12RB1* exons 9, 9b and 10, as well as their intervening introns. The sequences of p*B1*$^{9–10}$ and p*B1*$^{9–11}$ are identical, with the exception that exon 11 is absent from p*B1*$^{9–10}$; also depicted are the splicing patterns of p*B1*$^{9–10}$-derived Iso1 mRNA (pink dotted line) and p*B1*$^{9–10}$-derived Iso2 mRNA (brown solid line). Deletion mutant derivatives of p*B1*$^{9–10}$ were generated and include: ΔpolyA, which lacks 345 nt encompassing the *IL12RB1* exon 9b polyadenylation site and a portion of the downstream intron; ΔpolyAΔex10, which eliminates the *IL12RB1* exon 9b polyadenylation site region through *IL12RB1* exon 10; Δex9b, which is a 991 nt deletion that removes *IL12RB1* exon 9b and flanking intron sequences; Δex10, which lacks *IL12RB1* exon 10 and upstream intron sequences; vector alone, which contains no *IL12RB1* exons or introns. (**C**) Jurkat T cells were transfected with either p*B1*$^{9–10}$, p*B1*$^{9–11}$ or empty vector, and then cultured in the presence (+) or absence (-) of PHA; minigene-derived Iso1 and Iso2 expression was assessed 2 days later. Shown are the electrophoresis patterns of (*lane 1*) a ladder control, and amplicons from (*lane 2*) non-RT treated RNA, (*lane 3-4*) cells transfected with p*B1*$^{9–10}$, (*lanes 5-6*) cells transfected with

p*B1*$^{9–11}$, and (*lane 7*) cells transfected with empty vector. Arrows on the left indicate which amplicons correspond to p*B1*$^{9–10}$-derived Iso1 and Iso2 mRNA; arrows on the right indicate which amplicons correspond to p*B1*$^{9–11}$-derived Iso1, Iso1Δex10 and Iso2 mRNA. (**D**) Jurkat cells were transfected with either p*B1*$^{9–10}$ or a p*B1*$^{9–10}$ mutant; minigene-derived Iso1 and Iso2 expression was assessed 2 days later. Shown are the electrophoresis patterns of (*lane 1*) a ladder control, and amplicons from (*lane 2*) mock-transfected cells, and cells transfected with either (*lane 3*) empty vector, (*lane 4*) p*B1*$^{9–10}$, (*lane 5*) ΔpolyA, (*lane 6*) ΔpolyAΔex10, (*lane 7*) Δex9b, and (*lane 8*) Δex10. The gel image was cropped between *lane 1* and *lane 2*; arrows indicate which amplicons correspond to minigene-derived Iso1 and Iso2 mRNA.

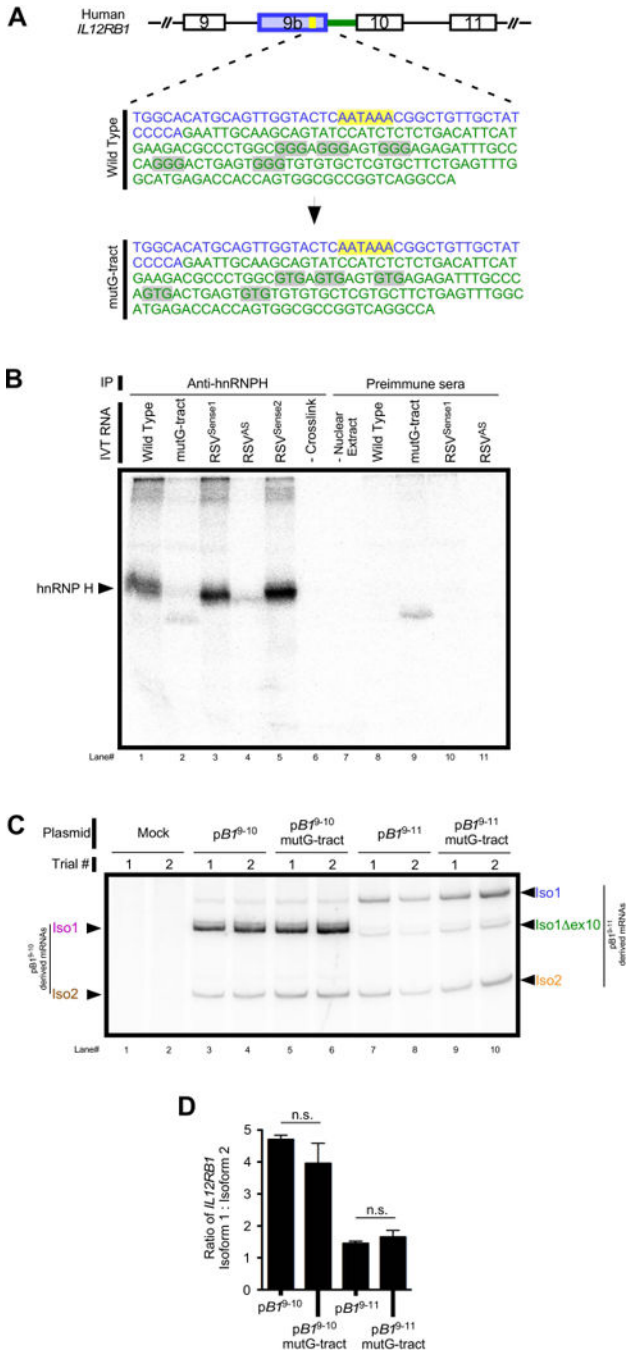

FIGURE 5.

hnRNP H physically associates with *IL12RB1* mRNA in a G-tract dependent manner. (**A**). Putative hnRNP H binding sites are located in the intron between exons 9b-10 (gray highlight) and comprises five GGG repeats (G-tracts). The exon 9b polyadenylation signal (yellow highlight) and 3' RNA terminus (blue) are shown for reference. Green denotes intron sequence. *IL12RB1* minigenes were generated in which all five G-tracts were mutated from GGG (wild type) to GTG (mutG-tract). (**B**) To determine if hnRNP H physically associates with *IL12RB1* pre-mRNAs at these sites, radiolabeled transcripts containing wild type (lane

1) or mutant (lane 2) *IL12RB1* G tracts were incubated in HeLa nuclear extract, UV cross-linked, immunoprecipitated with anti-hnRNP H, and resolved using SDS-PAGE/autoradiography. RSV^{Sense1} (lane 3) and RSV^{Sense2} (lane 5) are positive control RNAs known to bind hnRNP H[58]; the antisense of RSV^{Sense1} served a negative control (RSV^{AS}, lane 4). Additional controls include wild type *IL12RB1* RNA that was not crosslinked prior to immunoprecipitation (–Crosslink, lane 6), and a control reaction containing no HeLa nuclear extract (lane 7). Lanes 8-11 are control reactions immunoprecipitated using a nonspecific preimmune sera. (**C**) Jurkat cells were transfected with either p$B1^{9–10}$, p$B1^{9–10}$mutG-tract, p$B1^{9–11}$, or p$B1^{9–11}$mutG-tract (a derivative of p$B1^{9–11}$ harboring mutant G-tracts); minigene-derived Iso1 and Iso2 expression was assessed 2 days later by semi-quantitative PCR. Arrows on the left indicate which amplicons correspond to p$B1^{9–10}$-derived and p$B1^{9–10}$mutG-tract-derived Iso1 and Iso2 mRNA; arrows on the right indicate which amplicons correspond to p$B1^{9–11}$-derived and p$B1^{9–11}$mutG-tract-derived Iso1 and Iso2 mRNA. (**D**) Quantitation of the above semi-quantitative PCR.

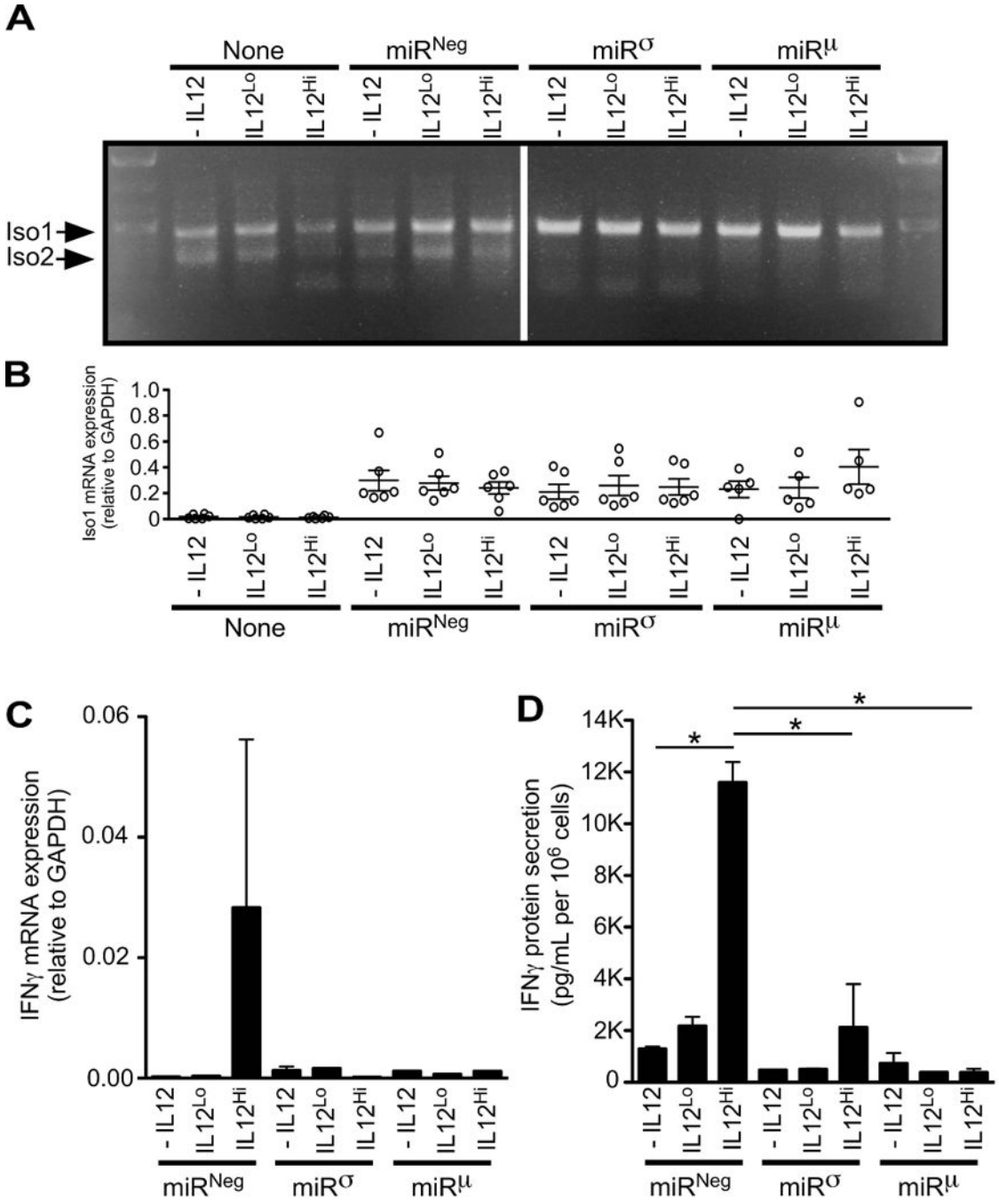

FIGURE 6.

Human *IL12RB1* Isoform 2 positively regulates IL12-dependent IFNγ expression. Jurkat T cells were transduced via lentivirus with one of two microRNAs (miR$^{\sigma}$ and miR$^{\mu}$) designed to knockdown *IL12RB1* Isoform 2 expression, without affecting *IL12RB1* Isoform 1. The design and validation studies of miR$^{\sigma}$ and miR$^{\mu}$ are shown in FIG S1; the lentiviral vector used for miR transduction also encoded GFP. Control Jurkat T cells were either left non-transduced (none), or transduced with a microRNA that does not target any human gene (miR^{Neg}). GFP+ transductants were sorted and cultured in the presence of PHA and 3

different IL12 concentrations (-IL12, $IL12^{Lo}$ and $IL12^{Hi}$). The cells in each culture condition were collected 2 days later, counted and used for (**A-C**) mRNA expression studies; cell supernatants were collected at the same time and used for (**D**) IFNγ ELISA measurements. (**A**) Multiplex amplification of Isoform 1 (Iso1) and Isoform 2 (Iso2) mRNA from stimulated miR-transductants. Shown is an agarose gel image that was used to visually confirm the knockdown of Iso2 in miR^{σ}- and miR^{μ} -transduced cells, relative to both non- or miR^{Neg}-transduced cells **(B)** qRT-PCR measurement of Isoform 1 mRNA expression, as normalized to the GAPDH expression in the same cell preparations. Each open circle represents the data from an individual experimental replicate (6 experimental replicates per condition). **(C)** qRT-PCR measurement of IFNγ mRNA expression, as normalized to the GAPDH expression in the same cell preparations. Shown are combined data from all 6 experimental replicates. **(D)** IFNγ levels in the supernatants of stimulated miR-transductants, as normalized to cell count. Shown are combined data from all 6 experimental replicates; *, $p<0.05$ as determined by ANOVA analysis.

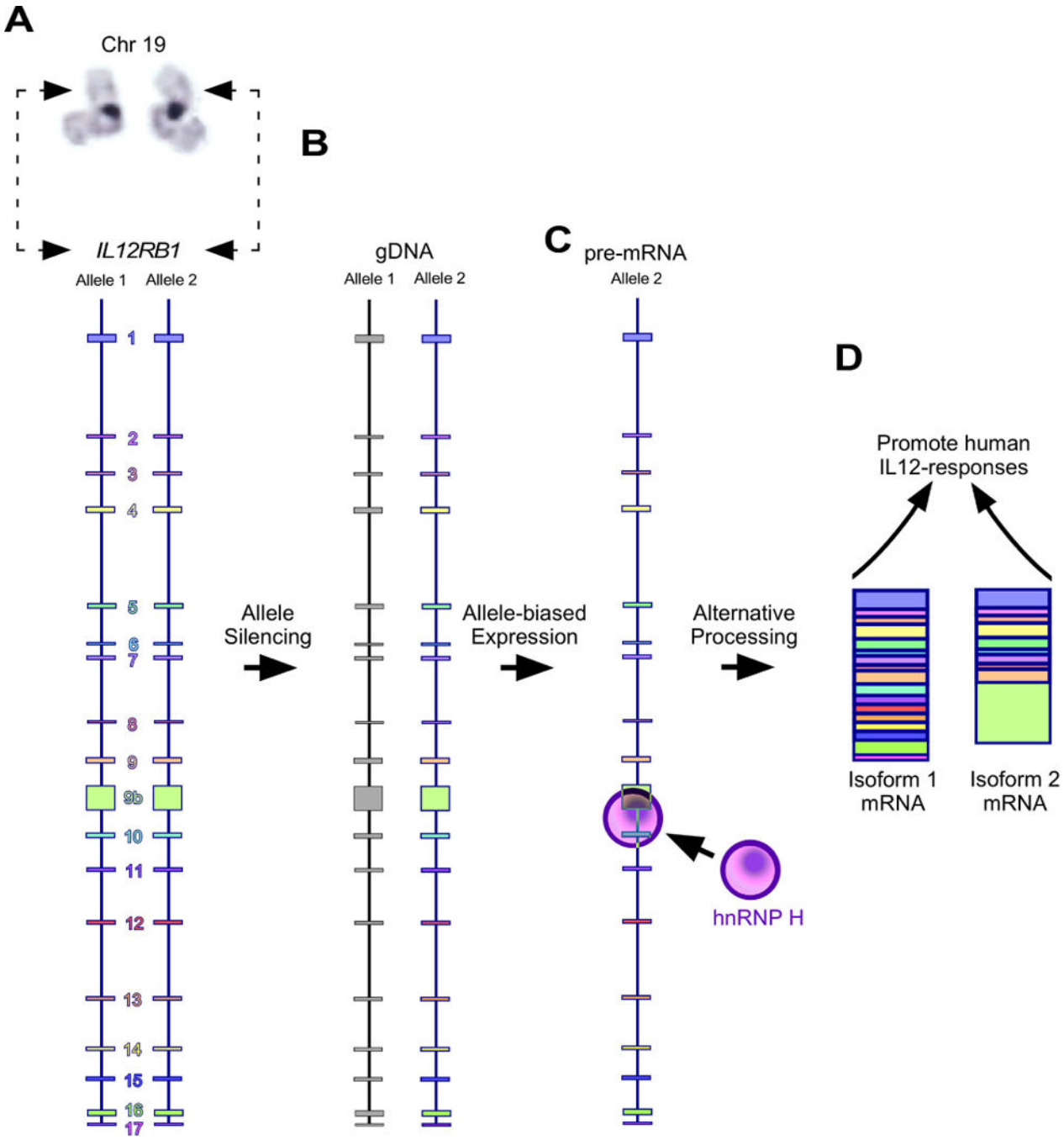

FIGURE 7.

Model of *IL12RB1* allele expression, processing and isoform function. **(A)** Human *IL12RB1* is located on the p-arm of chromosome 19, and comprises exons 1-9, 9b, and 10-17. Shown is a karyotype image of chromosome 19, with the hatched arrows indicating the approximate position of *IL12RB1*. Depicted along the length of each *IL12RB1* allele are the location and relative sizes of each exon and intron. **(B)** In primary human tissue, one *IL12RB1* allele is silenced (represented by the gray exons of Allele 1) while and the other is transcriptionally active (represented by the colored exons of Allele 2). **(C)** The active allele is transcribed into

a *IL12RB1* pre-mRNA, which binds hnRNP H via G-tracts that are downstream of the Exon 9b poly(A) site. **(D)** The *IL12RB1* pre-mRNA is the alternatively spliced into either Isoform 1 or Isoform 2, both of which promote IL12 responses.